S. MAZZOLI(*)

# STRUCTURAL ANALYSIS OF THE MESOZOIC LAGONEGRO UNITS IN SW LUCANIA (SOUTHERN ITALIAN APENNINES)(**)

CONTENTS




## ABSTRACT

This study discusses the structural analysis of the tectonic units outcropping in the Lagonegro Zone of SW-Lucania (southern Italy). The Mesozoic sediments of the Lagonegro and adjacent nappes have undergone a polyphase deformation history, which is superposed on an already complicated Middle Triassic to Lower Cretaceous palaeotectonic evolution. Field mapping and structural analysis revealed two main contractional deformation sequences in the Lagonegro nappes. During the early stages of the $D_1$ deformation sequence, the Mesozoic sediments of the Lagonegro basin were detached from their substratum. Continued NE-directed thrusting (in present-day co-ordinates) led to nappe formation and to the regional juxtaposition of Lagonegro Unit II over Unit I. Main folding within the two nappes was essentially coeval with nappe emplacement. Further thrusting occurred within Lagonegro Unit I, involving faulting of already folded rocks with only limited displacements compared to the main nappe transport. The fold geometry appears to have been often modified by movement over the thrust surfaces: folds tighten and axial planes make progressively lower angles with the thrust towards the thrust tip-line. A discontinuously developed slaty cleavage ($S_1$) formed in the less competent lithologies during this deformation sequence. Refolding of the whole tectonic pile occurred as a consequence of (present-day) N-S to NNE-SSW shortening ($D_2$). In the less competent lithologies, a crenulation cleavage ($S_2$), usually in the form of conjugate kink bands, is associated with this deformation. Refolding produced different types of interference structures at various scales. The most commonly observed are transitional forms between Type 1 and Type 2 interference patterns. Although these complex structures never represent simple type end-members, at a first approximation a pattern can be recognized consisting of (dominant Type 1) dome-like structures developed on early broad anticlines and of (dominant Type 2) tight synclinal structures with folded axial surfaces developed on early "pinched" synclines.


(*)ETH Zentrum - Zürich.

(**)Contribution n. 1 of the italian C.N.R. Research Project "Geodynamics and Active Tectonics of the Tyrrhenian Apennine System" (Resp. F.C. WEZEL).


## RIASSUNTO

In questo lavoro vengono presentati i risultati dell'analisi strutturale delle unità tettoniche Lagonegresi nell'area di Lagonegro - Monte Sirino (Basilicata sud-occidentale). Il rilevamento geologico-strutturale è stato effettuato alla scala 1:10.000, cartografando i singoli affioramenti; una versione semplificata (alla scala 1:25.000) della carta geologica è allegata a questo lavoro.

Due principali deformazioni compressive sono state distinte sulla base dell'analisi strutturale. La prima di esse ($D_1$) non costituisce una singola fase di deformazione discreta, bensí una serie di eventi deformativi costituiti da sovrascorrimenti e deformazione interna delle falde, con generale vergenza verso l'avampaese apulo (NE in coordinate odierne). Detta "sequenza deformativa" ($D_1$) consiste nello scollamento dei sedimenti del bacino di Lagonegro dal loro basamento e nella formazione delle principali falde lagonegresi ad estensione regionale. Una prima fase di piegamento nelle falde lagonegresi risulta essere essenzialmente coeva con la messa in posto delle falde stesse, come dimostrano i rapporti geometrici tra le pieghe e le principali superfici di sovrascorrimento. Sovrascorrimenti di minore entità (*break thrusts*) all'interno dell'unità tettonica inferiore (Lagonegro I) tagliano le pieghe già formate. La geometria delle pieghe appare essere modificata dal movimento sulla superficie di thrust: esse diventano progressivamente piú chiuse e rovesciate (fino a coricate) verso la parte frontale dei sovrascorrimenti. Una foliazione ($S_1$) di tipo *slaty cleavage*, sviluppata in maniera discontinua nell'area rilevata, è associata alle pieghe $F_1$ nelle litologie incompetenti.

Un successivo raccorciamento ($D_2$), con orientazione da N-S a NNE-SSO (in coordinate odierne), è responsabile del ripiegamento delle unità lagonegresi. Un clivaggio di crenulazione ($S_2$), nella maggior parte dei casi sviluppato in forma di *kink bands* coniugati, è associato a questa deformazione nelle litologie meno competenti. Il piegamento sovrapposto ha prodotto vari tipi di strutture d'interferenza a diverse scale. Quelle piú frequentemente sviluppate sone forme di transizione tra le geometrie d'interferenza di Tipo 1 e di Tipo 2. Nonostante queste siano strutture complesse che non costituiscono mai semplici *patterns* puramente dell'uno o dell'altro tipo, in prima approssimazione è possibile distinguere due modalità principali di sovrapposizione delle strutture plicative: strutture a domo (o di predominante Tipo 1) tendono a svilupparsi sulle ampie anticlinali di prima fase, mentre strutture di predominante Tipo 2, con superfici assiali ripiegate, tendono a svilupparsi sulle strette sinclinali di prima fase. Il piegamento sovrapposto è responsabile, almeno in parte, degli accentuati andamenti arcuati delle strutture osservabili dalla carta geologica.

KEY WORDS: Structural analysis, Superposed deformations, Lagonegro area, southern Apennines.

PAROLE CHIAVE: Analisi strutturale, Deformazioni sovrapposte, Area di Lagonegro, Appennino meridionale.

## INTRODUCTION AND REGIONAL SETTING

The Lagonegro area, situated in the Lucania region SE of Naples (Fig. 1), represents a key area for the understanding of the palaeogeographic and tectonic evolution of the southern Apennines and, more generally, of the whole peri-Adriatic region. In this area, Mesozoic basin sediments as old as Middle Triassic outcrop within a series of thrust sheets which are part of the deformed remnants of the southern continental margin of the Jurassic - Early Cretaceous Neoethyan ocean (e.g. LAUBSCHER & BERNOULLI, 1977; CHANNELL *et alii*, 1979; ROURE *et alii*, 1991). Mesozoic deep water deposits resembling those of the Lagonegro Zone, pelagic limestones, radiolarian cherts and carbonate turbidites - sometimes associated with submarine volcanics - are known from many places along the Alpine-Himalayan chain (BERNOULLI & JENKYNS, 1974). Discontinuosly preserved remnants of such basins can be traced from Sicily (Sclafani Zone and Monti Sicani) and the Lagonegro Zone in southern Italy through Greece (Pindos), southern Turkey (Antalaya nappes), Cyprus (Mamonia Complex), Iran (Pichakun Zone), and Oman (Hawasina nappes) (BERNOULLI *et alii*, 1990 and references therein). They are interpreted to record the existence of a Triassic seaway between the extensive carbonate platforms bordering the northern margin of Gondwana (SCANDONE 1975a). The basement of these Triassic basins is unknown; for the eastern occurrences (Hawasina Basin) at least, a Permo-Triassic oceanic basement is advocated (STAMPFLI *et alii*, 1991).

In the present-day geometry of the southern Apennines, the units derived from the Lagonegro basin tectonically overlie units of the Apulia Platform of the geological literature (eastern platform in Fig. 1), and are themselves overlain by units derived from the more internal "Apenninic Platform" (western platform in Fig. 1) (e.g. MOSTARDINI & MERLINI, 1986). The entire sequence is capped by thrust sheets derived from more internal domains, which include the Liguride Complex, flysch deposits of Neotethyan origin with incorporated oceanic slices (KNOTT, 1987), and, more to the south, the Calabrian nappes, units with a continental base-

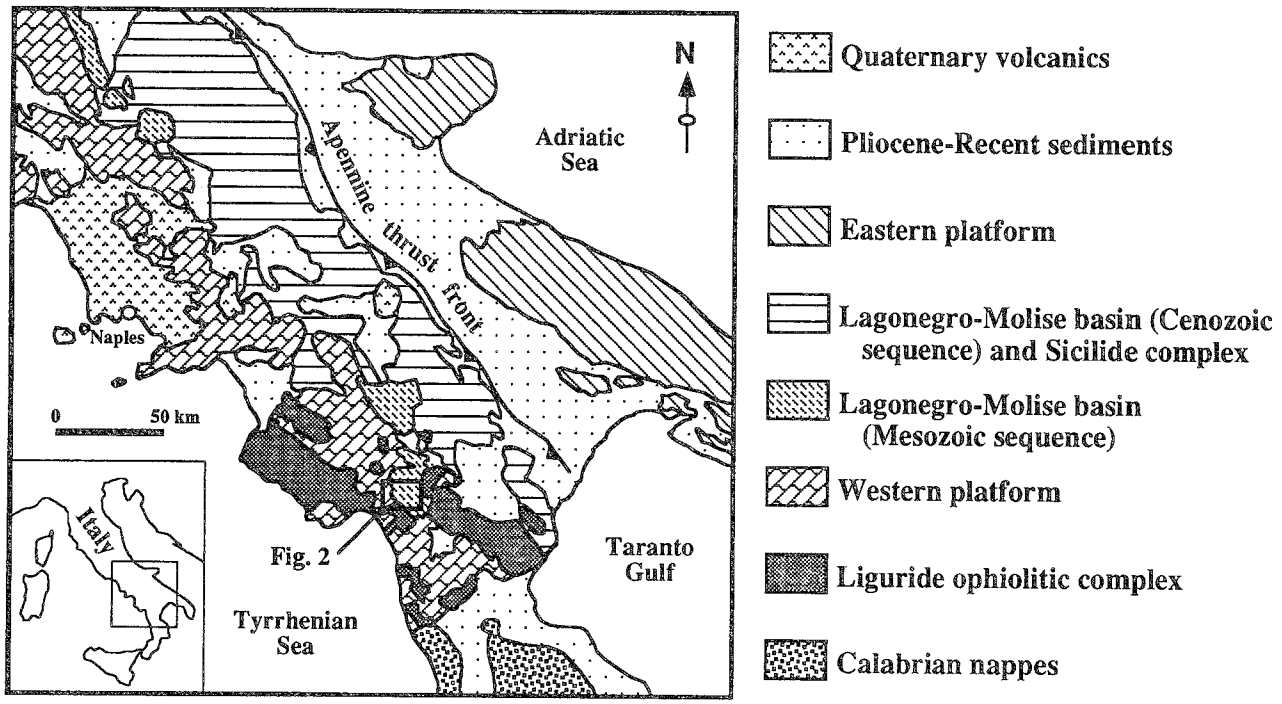


Fig. 1 - Geologic map of the southern Apennines showing the main tectonostratigraphic units (after ROURE *et alii* 1991, modified) and location of the study area.

ment considered to be remnants of the European plate (i.e. north Tethyan margin; e.g. OGNIBEN, 1969; BOUILLIN *et alii*, 1986; DIETRICH, 1988).

In the investigated area (Fig. 2), the units derived from the Lagonegro basin outcrop in a tectonic window formed in correspondence of a culmination which developed as an antiformal stack of the buried carbonate thrust sheets (CINQUE *et alii*, in press). Relatively good surface outcrop over ca. 1500 m of vertical relief formed the basis from which a carefully constrained three-dimensional picture could be constructed. It shows a polyphase history consisting of a sequence of thrusting events propagating towards the Apulian foreland with associated internal deformation within the thrust sheets ($D_1$), followed by later refolding ($D_2$) involving considerable distortion of the already formed structures (MAZZOLI, 1993a). The main tectonic framework suggested by SCANDONE (1967, 1972), consisting of two superposed nappes consisting of Mesozoic Lagonegro basin sediments, is confirmed in the study area. The two Lagonegro nappes are characterised by well defined, different but clearly correlatable, Upper Triassic to "middle" Cretaceous stratigra-

phies (summarised in Figs. 2 & 3). The oldest deposits of the basin, those of the Middle Triassic Monte Facito Formation, only outcrop at the base of the upper nappe, but it is probable that similar successions originally underlay the entire basin (e.g. WOOD, 1981). The structurally upper nappe (Lagonegro Unit II) displays more proximal basin facies, while the lower nappe (Lagonegro Unit I) shows more distal, deep basin facies. The thrust contact between the two units can be observed at different localities, where kinematic indicators are also sometimes present. It represents a main structural feature of the study area, leading to a tectonic juxtaposition of different depositional areas on at the scale 1:10,000, distinguishing exposed from unexposed regions and observed from inferred contacts. A simplified (1:25,000) version of the geological map with profiles is included in this paper. Most of the area mapped in the present study consists of Mesozoic terranes of the two Lagonegro units. In the western sector, structurally higher thrust sheets of the M. Foraporta Unit and derived from the western carbonate platform (Alburno-Cervati Unit) also outcrop (Fig. 2). Four geological profiles - originally constructed at the scale 1: 10,000 - across the study area are shown in Fig. 4. The terminology used in the text is shown in the geological map of Fig. 2.

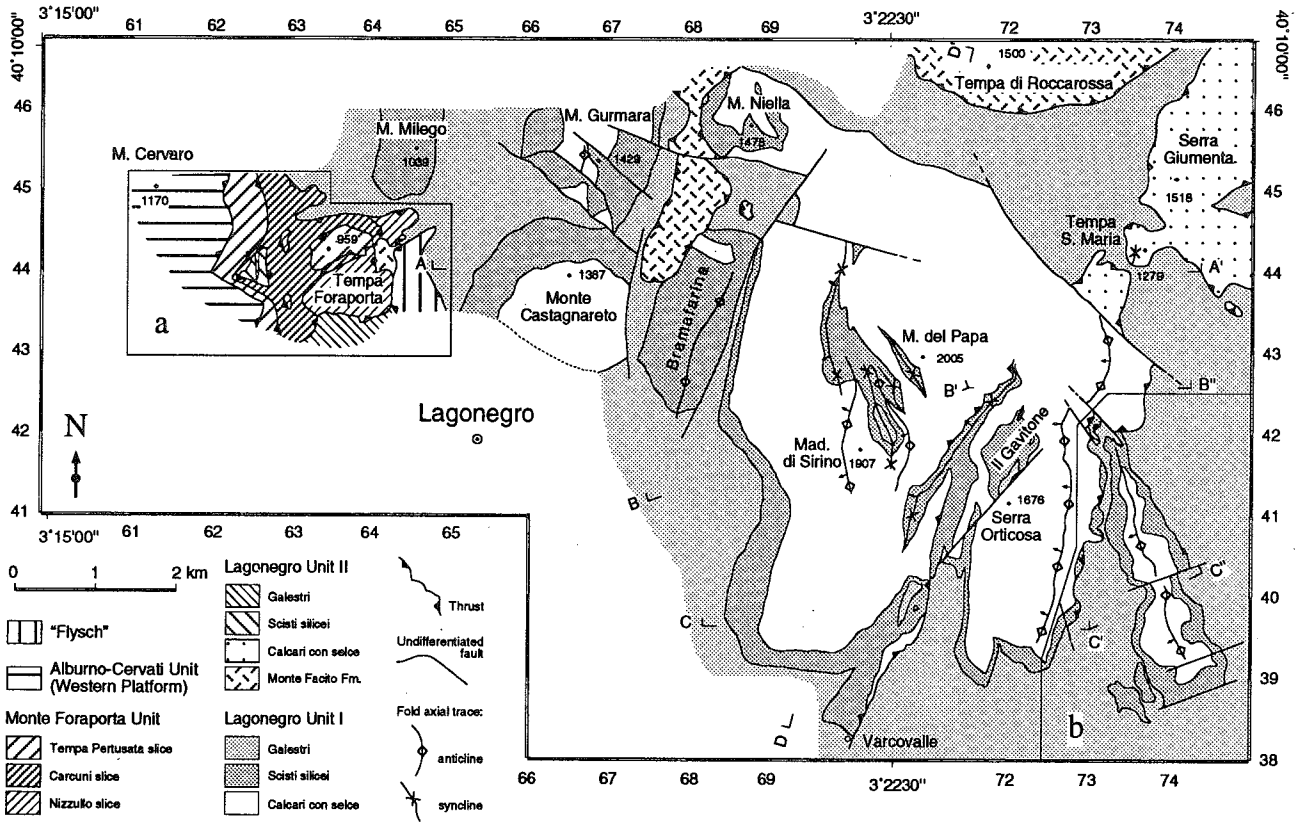


Fig. 2 - Geological map of the study area showing terminology used in the text and location of the cross-sections of Fig. 4. Geographic co-ordinates refer to the International Ellipsoid oriented in Rome (M. Mario). Kilometric grid of the "Foglio 210 della Carta d'Italia" also shown. Framed area (a) partly after DE ALFIERI *et alii* (1986), framed area (b) partly after TORRENTE (1990).
Alburno-Cervati Unit (western platform): neritic limestones, dolomitic limestones and dolomites (Upper Triassic - Miocene). Monte Foraporta Unit: Tempa Pertusata slice: limestones, marly limestones, marls and shales (Liassic - Dogger); Carcuni slice: black dolomites (Upper Triassic? - Lower Liassic?); Nizzullo slice: white to grey dolomites (Upper Triassic?). Lagonegro Unit II: Galestri: alternating argillites, marls, graded calcarenites and calcilutites (Lower Cretaceous); Scisti silicei: polychrome radiolarites and siliceous argillites with rare intercalations of (mostly silicified) graded calcarenites (Jurassic); Calcari con selce: intraformational conglomerates, grey calcilutites with bands and nodules of chert (Norian - carnian); Monte Facito Fm.: shales interbedded with shallow-water calcarenites and calcisiltites, siltites and micaceous sandstones, olistoliths of massive neritic limestone. Lagonegro Unit I: Galestri: alternating dark argillites and strongly siliceous calcilutites (Lower Cretaceous); Scisti silicei: polychrome radiolarites and siliceous argillites (Middle Tithonian - Upper Norian); Calcari con selce: calcilutites with bands and nodules of chert (Norian *p.p.* - Carnian) As "Flysch" are indicated chaotic terranes (outcropping around the town of Lagonegro) consisting of argillites containing disrupted sandstones, calcilutites, cherts, microbreccias with nummulites, *Lepidocyclina, Amphistegina, Miogypsina.*

a regional scale. The definition of two Lagonegro nappes therefore appears to be appropriate and is maintained in this work.

In this paper, the main results of the structural analysis based on field observations are presented. Geological mapping of the study area has been carried out

## STRUCTURAL ELEMENTS OF THE MAIN ($D_1$) DEFORMATION SEQUENCE

$D_1$ does not represent a single discrete deformation phase, but rather a sequence of thrusting events accompanied by internal deformation within the thrust

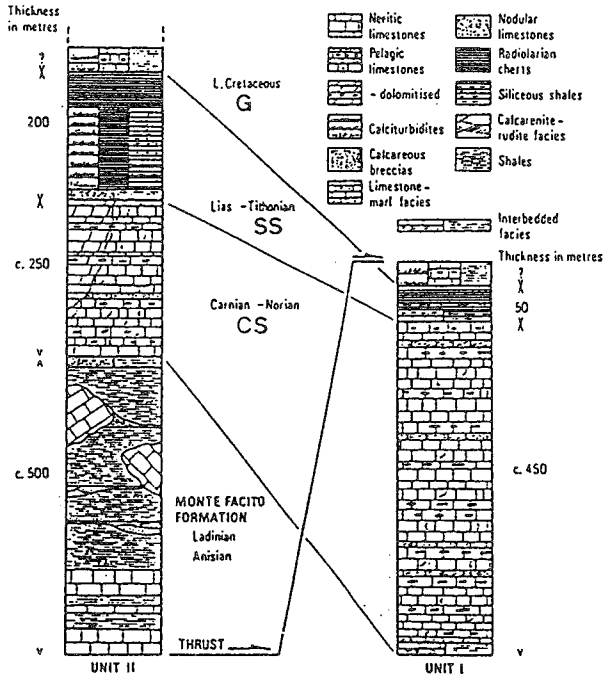


Fig. 3 - Stratigraphy of the Lagonegro Zone (after WOOD 1981, slightly modified). CS = "Calcari con Selce", SS = "Scisti Silicei", G = "Galestri". Cherts and siliceous shales of Senonian age have been described on top of Unit I ("Red Shales of Pecorone"), while Upper Cretaceous - Miocene "Flysch Rosso", comprising a variety of pelagic and redeposited shallow-water lithologies, may conformably overlie the "Galestri" in Unit II. Otherwise, no deposits younger than Lower Cretaceous are preserved.

sheets. The deformation sequence includes nappe emplacement, main folding within the nappes and further thrusting in the lower nappe. All these features appear to be geometrically closely related, and probably resulted from continuing deformation with a general Apulian (NE in present-day co-ordinates) vergence.

*Lagonegro Unit II*

The upper Lagonegro nappe (Unit II) is only exposed in a few small areas of the mapped region (Fig. 2). The Middle Triassic M. Facito formation outcrops in the NE sector of the study area (Tempa di Roccarossa) and forms an approximately N-S oriented tongue between the ridges of M. Gurmara - M. Castagnareto and M. Niella - Bramafarina. To the east, the Upper Triassic "Calcari con selce" of Unit II lie directly above the thrust surface (klippe of Serra Giumenta). A late normal fault brings part of these limestones into contact with the "Calcari con selce" of the underlying Lagonegro I nappe SW of Tempa S. Maria.

The thrust surface at the base of Unit II is generally gently bowed and is discordant with the structures in the footwall; locally it also exhibits out-of-sequence thrust relationships, as may be observed east of M. Castagnareto where it cuts down-section in the footwall in the direction of transport (cf. profile A-A', Fig. 4). These observations contrast with those of SCANDONE (1967, 1972), who describes a thrust contact conformably folded with the structures within the nappes. On the basis of such geometrical relationships, Scandone suggested that early nappe emplacement was followed by folding of the already imbricated sheets and of the interposed thrust surface.

Relatively good, although discontinuous outcrops of limestones with cherts in the klippe of Serra Giumenta allow observation of the internal structures of the upper Lagonegro nappe. Folds within the klippe are generally gently plunging, with wavelengths of a few tens of meters to about 100 m. Metric-scale parasitic folds are common, and show typical symmetric (*m*) or asymmetric (*s* or *z*) shapes depending on their structural position. A continuous transition can be observed from gently inclined or even recumbent tight folds (with sharp hinges) at the base of the nappe, to more inclined and upright open folds (with rounded hinges) moving upwards away from the thrust surface (Figs. 5, 6 & 7). Axis azimuths vary from N-S to NE-SW (Fig. 8a-c). A consistent departure from the cylindrical fold geometry (defined according to RAMSAY & HUBER, 1987) is shown by the structure of Serra Giumenta (Fig. 8b). The non-cylindrical geometry at Serra Giumenta is at least in part due to later refolding, as moderately inclined, roughly E-W trending, gentle to open folds of metric amplitude are observed in the limbs of the major structure. All fold axes are oblique to the thrusting direction as determined at Tempa S. Maria (Fig. 5); most of them lie within few tens of degrees to the mean transport direction (Fig. 8c).

At Tempa di Roccarossa (Fig. 2), the Middle Triassic M. Facito Fm. (Lagonegro Unit II) tectonically overlies Lower Cretaceous argillites and interbedded limestones ("Galestri") of Unit I (Fig. 9). The M. Facito Fm. contains in this area a large neritic limestone block of kilometric size resting above mainly terrigenous sediments (Terrigenous Clastic Facies of WOOD, 1981). The latter comprise shales (mainly quartzose and subordinate calcareous mudstones and siltstones) and poorly-exposed, fine- to medium-grained micaceous sandstones. Scattered outcrops of shallow-water limestones (Neritic Limestone Facies of WOOD, 1981) are also observed around the base of Tempa di Roccarossa. All these lithologies show gently inclined to recumbent tight folds and a flat lying cleavage in the incompetent beds (Fig. 10). Incompetent layers show class 3 fold geometries (RAMSAY, 1967), while competent beds display class 1B or class 1C shapes. Such thickness variations of the competent and incompetent layers, together with the cleavage pattern in the folds (divergent fans in the incompetent beds, convergent fans, when developed, in the competent ones) strongly suggest an origin of the folds by buckling mechanisms (cf. RAMSAY, 1981, 1989), that is the sideways deflection of a mechanically unstable competent layer into neighbouring incompetent rock as a result of layer shortening.

*Discussion.* - The transition from upright to recumbent folding, with tightening of folds accompanying the decreasing dip of the axial plane as observed in the klippe of Serra Giumenta, is relatively common in thrust sheets and high-level nappes (cf. SANDERSON, 1982). According to this author, this feature characterises sheets emplaced by heterogeneous simple shear (with shear strain $\gamma \approx 0$ in the upper parts of the sheet, increasing downwards toward the thrust surface) associated with a component of layer parallel shortening (Fig. 11). It must be noted that the combination of strains shown in Fig. 11b is compatible in nappes and thrust sheets as these are not subject to the constraint of continuity of strain (cf. RAMSAY & GRAHAM,

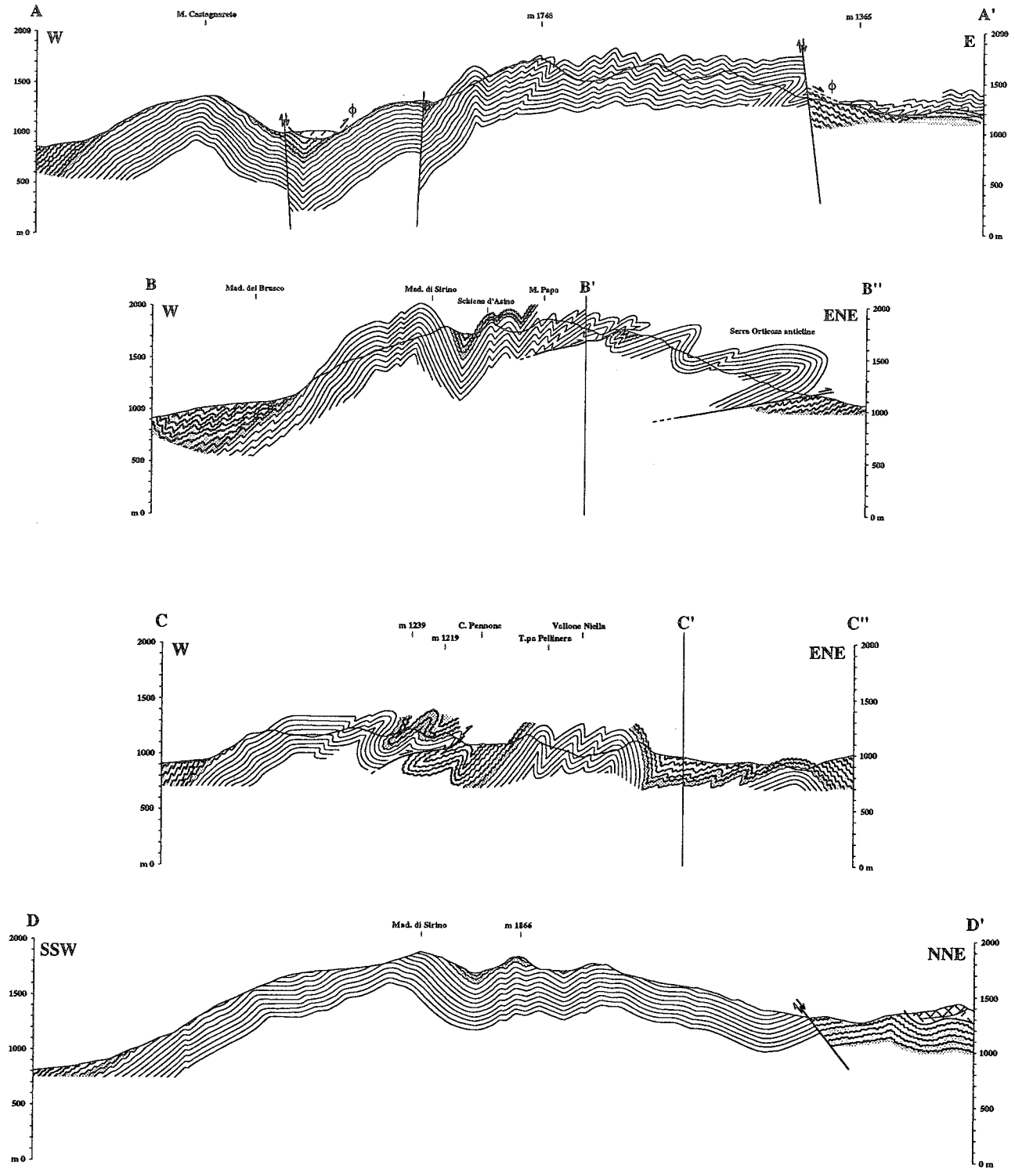


Fig. 4 - Geological cross-sections (location in Fig. 2). In profile A-A', $\phi$ is the main thrust between Lagonegro Unit II and Lagonegro Unit I.

1970) across the thrust plane, which represents therefore an "incoherent strain domain boundary" (MEANS, 1976).

The geometry of folds at the base of Tempa di Roccarossa, showing shallow-dipping axial planes and tight shapes (Fig. 10), is probably also due to the effect of high shear strain near the sole of the nappe. Such a shear strain may also account for the pattern of extension veins and boudinage locally observed in the folded limestones (Fig. 12). The inferred strain history is very similar to that described by RAMSAY *et alii* (1983) for the simple shear deformation of a competent layer initially oriented at a low angle to the shear plane (Fig. 13). During initial folding, the layer lies in the shortening field of the strain ellipse for the simple shear deformation. During progressive simple shear, the fold limbs rotate toward the axial plane as the structure tightens (Fig. 13a). When the fold limbs take up

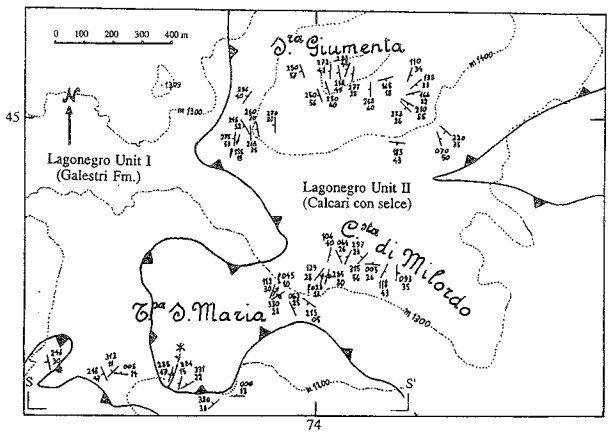


Fig. 5 - Geological map of the area of Serra Giumenta (kilometric grid of "Foglio 210 della Carta d'Italia"). Folds in the "Calcari con selce" of the Lagonegro Unit II are recumbent or gently inclined near the base of the nappe, and become progressivly more inclined moving upwards (axial surfaces are sub-vertical at Costa di Milordo). Asterisk (lower left corner) shows site from which thrust-related kinematic indicators were measured; S-S' shows trace of the cross-section of Fig. 6.

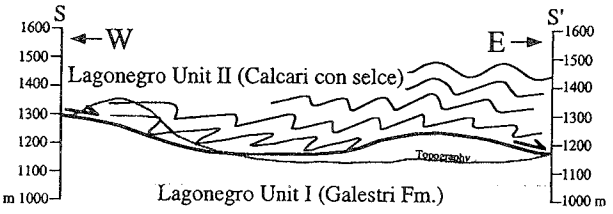


Fig. 6. Schematic cross-section showing the structure of the "Calcari con selce" in the klippe of Serra Giumenta. Note the decreasing dip of the fold axial surfaces towards the base of the nappe.

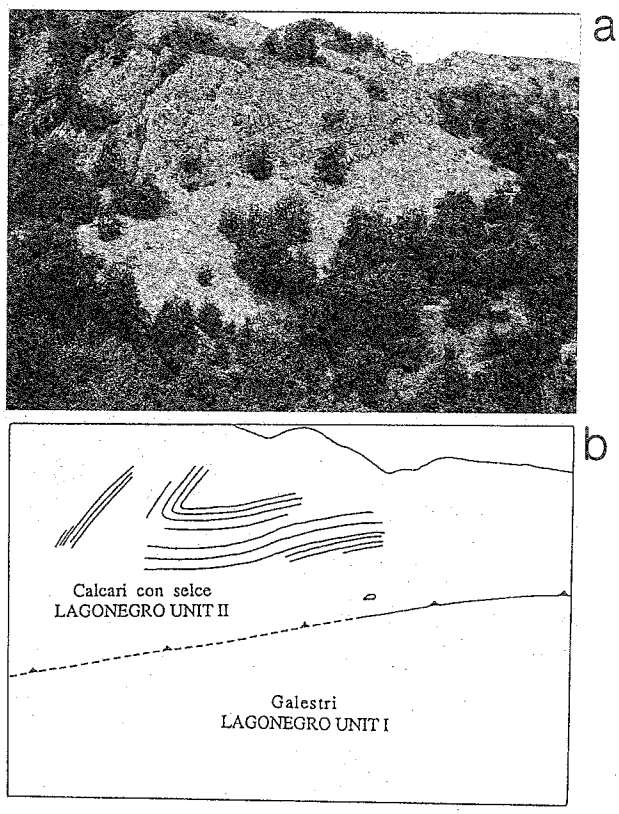


Fig. 7 - (a) Upper Triassic limestones ("Calcari con selce") of Unit II tectonically overlying dark argillites (Galestri Fm.) of Unit I at Tempa S. Maria (Fig. 5). Note gently inclined synclinal fold in the limestones above the thrust surface (E is to the right). (b) Line-drawing from (a).

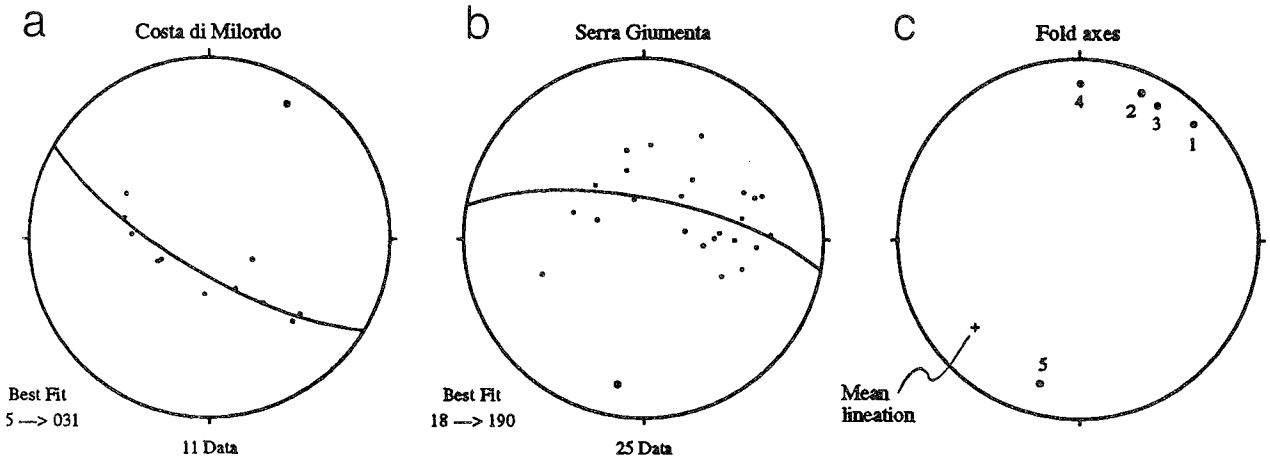


Fig. 8 - Orientation data for Serra Giumenta klippe (Lagonegro unit II): (a) Poles to bedding from open upright folds at Costa di Milordo; pole of the best great circle through the poles to bedding (cf. MANCKTELOW 1981) is also shown (larger dot). (b) Poles to bedding from upright structure at Serra Giumenta; pole of the best great circle through the poles to bedding is shown. (c) Fold axes orientations: 1, recumbent anticline at Costa di Milordo (base); 2, moderately inclined anticline at Costa di Milordo (intermediate); 3, pole of the best great circle through the poles to bedding of upright folds at Costa di Milordo (top); 4, gently inclined syncline at Tempa S. Maria; 5, steeply inclined anticline at Serra Giumenta. Mean thrust transport direction was determined from mineral fibre lineations and slip vectors normal to the intersection of s-c structures at Tempa S. Maria using Bingham statistics (cf. CHEENEY 1983); mean lineation plunges 26 towards 229.

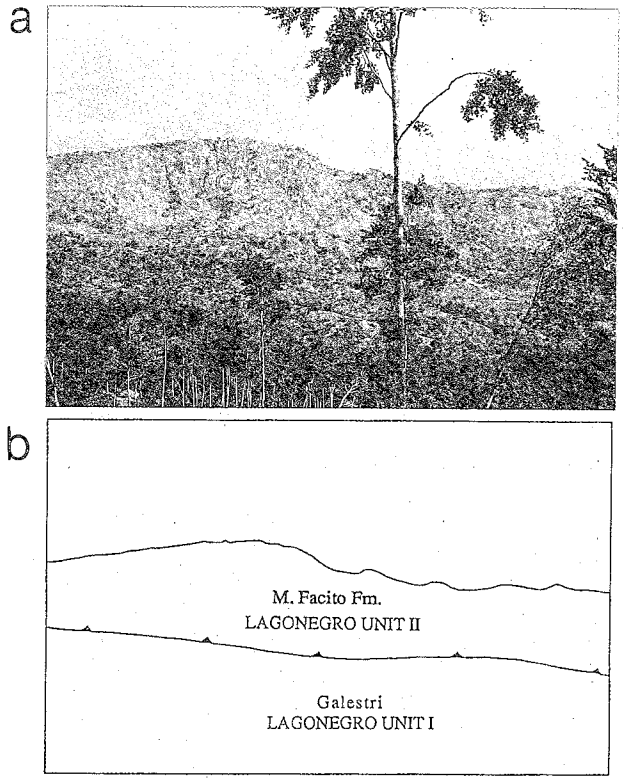


Fig. 9 - (a) Middle Triassic shallow-water limestone block of the M. Facito Fm. (Lagonegro Unit II) tectonically overlying Lower Cretaceous dark argillites of the Galestri Fm. (Unit I) at Tempa di Roccarossa. (b) Line-drawing from (a).

positions parallel or perpendicular to the shear plane (Fig. 13b), incremental shortening of the layer is instantaneously zero, but continued rotation of the fold limbs eventually brings them into the extensional field of the incremental strain ellipse (Fig. 13c). The required extension is accommodated in the present case by extensional veining and boudinage of the competent layers.

The orientation of the fold axes observed in the "Calcari con selce" of Serra Giumenta - oblique and mostly within a few tens of degrees of the measured direction of thrusting - is a feature commonly explained in simple shear deformation by the reorientation of folds initially formed sub-parallel to the Y axis of the strain ellipsoid by rotation towards the direction of transport, as originally suggested by BRIANT & REED (1969) for thrust sheets of crystalline rocks. According to ESCHER & WATTERSON (1974), this mechanism may also be important in moderately deformed supracrustal rocks, as are considered here. In simple shear, fold axes parallel to the Y axis would clearly show no tendency to reorientation if deformation was perfectly homogeneous. However, such a degree of homogeneity must be rare in nature, and differential flow is likely to realign fold axes sufficiently for reorientation to be accomplished by the homogeneous component of the deformation (ESCHER & WATTERSON, 1974). Furthermore, the very likely possibility of an original variability of fold axis attitudes greatly reduces the chances of individual folds being parallel to the Y direction (e.g. SANDERSON, 1973).

It must be noted that for the process described above, the strongest reorientation of fold axes would occur near the sole of the thrust sheet, where the shear

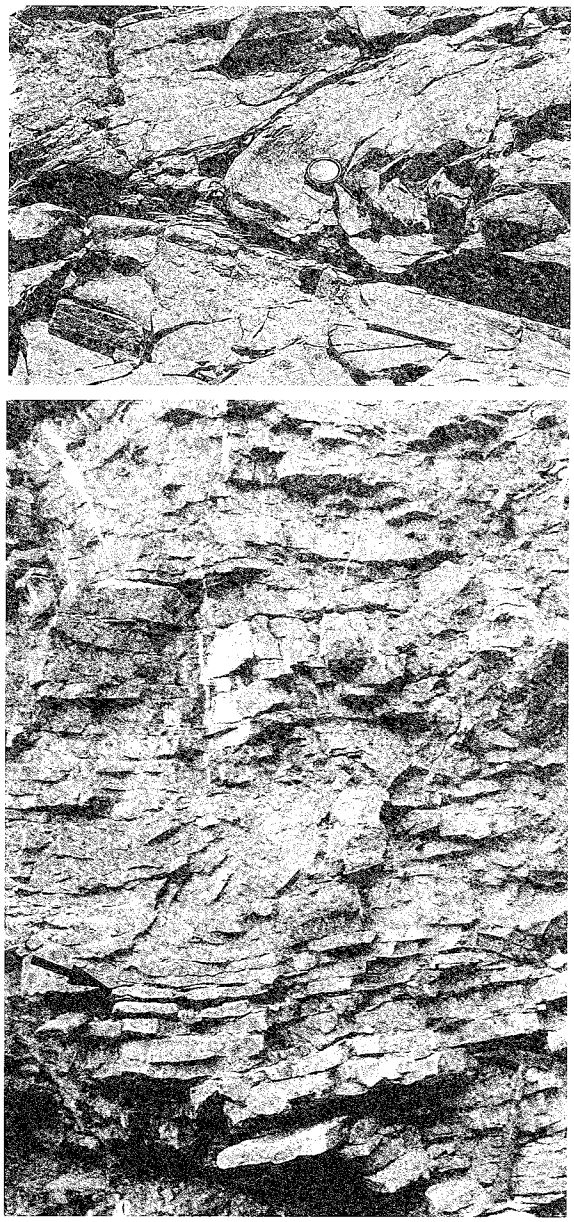


Fig. 10 - Folds in terrigenous sediments and in neritic limestones, lower part of the M. Facito Fm. (Middle Triassic) west of Tempa di Roccarossa (ENE is to the right of the pictures). (a) Recumbent folds in interbedded sandstones and shales. Note divergent cleavage fan in thin shaly layer and finite neutral point in the hinge zone. (b) Gently inclined asymmetric folds in limestones. Note extension veins and boudinage (arrowed) of the layers, showing extension parallel to bedding and normal to the fold axis.

strain $\gamma$ is maximum, and would then decrease strongly for the upper parts of the sheet where $\gamma$ is minimum. This leads to a fold axis orientation sub-parallel to the transport direction for tight recumbent folds at the base of the sheet and sub-pependicular to the thrusting direction for open upright folds, as shown by BRYANT & REED (1969) for the southern Appalachians. However, this feature is not observed in the present case. Open upright folds at Costa di Milordo show a very similar orientation to that of tight recumbent folds at the base of the nappe (Fig. 8c), both being close to the thrusting direction measured at Tempa S. Maria (cf. Fig. 5). On the other hand, the gently inclined syncline immedi-

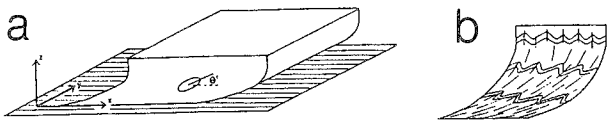


Fig. 11 - (a) Diagram of thrust sheet or nappe undergoing heterogeneous simple shear. (b) Profile of thrust sheet or nappe showing pattern of maximum strain trajectories (cleavage?) and folds for deformation occurring by heterogeneous simple shear and layer parallel shortening (from SANDERSON, 1982).

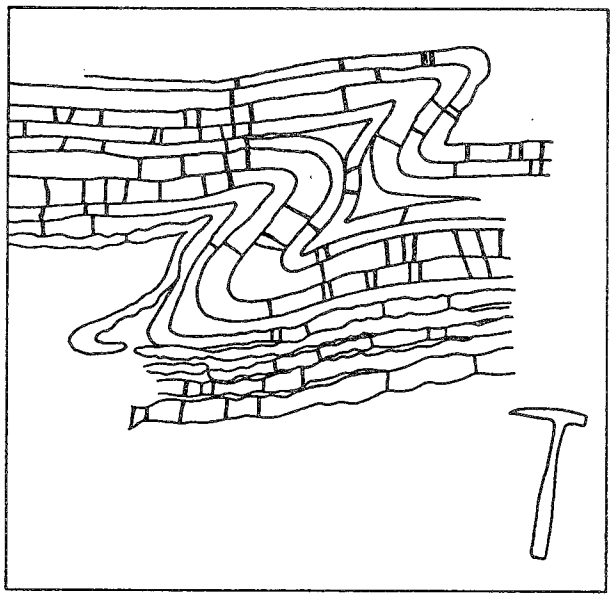

Fig. 12 - Sketch of the folds of Fig. 11b showing pattern of extension veins and boudinage.

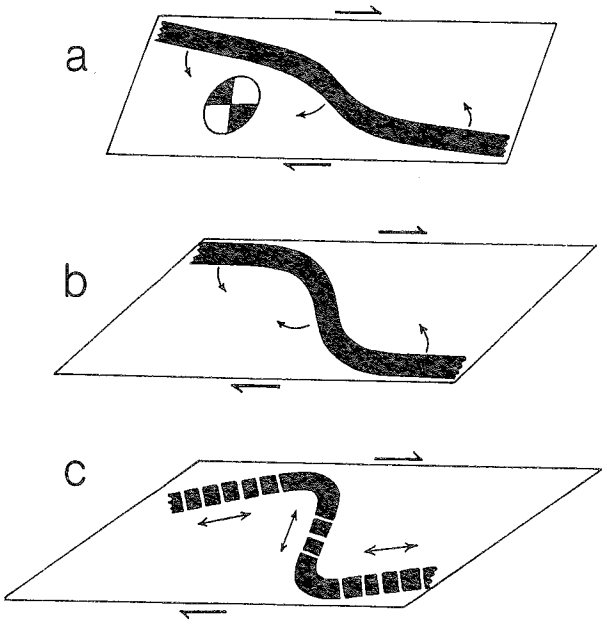


Fig. 13. - Strain history of buckled layers within a zone of simple shear (modified after RAMSAY *et alii*, 1983). Buckling leads to rotations of fold limbs (sense shown by curved arrows) and eventually to the rotation of fold limbs into positions where stretching takes place. Incremental strain ellipse for simple shear is shown with its field of extension (white) and shortening (dark).

ately above the thrust surface at the latter locality (Fig. 7) shows a quite different fold axis attitude - i.e. at a high angle (63) to the thrusting direction. Therefore, if a reorientation of the fold axes occurred in this area, it cannot be simply related to a shearing mechanism alone. As will be seen later on, late refolding at a high angle to the already formed structures may be partly responsible for the observed variability of both fold axes and axial trends of early-formed folds. In the present case, this possibility can be only tentatively suggested, as the very discontinuous outcrops do not allow the variations of structural trends between Tempa S. Maria, Costa di Milordo and Serra Giumenta to be followed in detail.

*Lagonegro Unit I*

Two-dimensional structural geometries of this nappe can be observed in profiles A-A', B-B'', C-C'' and D-D' of Fig. 4. Major folds within this unit are generally sub-horizontal to moderately plunging, upright to recumbent, and vary from open to tight. Folds of smaller (metric to decametric) wavelength have a polyharmonic interrelationship with major ones. Although often observed also in the Upper Triassic cherty limestones (''Calcari con selce''), they are particularly common in the Jurassic cherts (''Scisti silicei'') and in the alternating limestones and argillites of the Lower Cretaceous ''Galestri''. Mesoscopic ($F_1$) folds within the latter formation are open to tight, with half wavelengths of 0.5 - 10 m and amplitudes of 0.5 - 6 m. Fold geometry alternates between class 1 and class 3 (Ramsay 1967). Competent limestone layers have rounded hinges and show class 1b or class 1c geometries. Less competent argillites have angular to rounded hinges and typically exhibit class 3 geometries. Fold shape varies from symmetric and upright to asymmetric and overturned, with interlimb angles ranging from 12° to 95°. Striations and mineral fibre lineations, oriented at high angles to hinges, occur along bedding surfaces in Upper Triassic limestones and in Jurassic bedded cherts. Shear veins in limestones and in radiolarites consist of calcite and quartz fibres, respectively. They indicate a component of interlayer slip during folding.

*Cleavage.* - The main ($S_1$) cleavage is related to these fold structures. The cleavage is of disjunctive type - that is, cleavage domains, in contrast to crenulation domains, cut across pre-existing (sedimentary) layering in the rock without reorienting it (POWELL, 1979). Tectonic fabrics are best developed in the incompetent beds. Here, cleavage is mainly planar, morphologically ranging from the continuous (slaty) type to the spaced type and from a rough to a smooth variety (POWELL, 1979). In most of the cases, the cleavage lies at a low angle to bedding in the incompetent layers, almost irrespective of fold tightness (MAZZOLI & CARNEMOLLA, 1993). For this reason, due to the wide variability of fold limbs dip, the angle of dip of the cleavage is also quite variable. Strike orientation of cleavage planes are also variable across the region (cf. geological map). However, bedding-cleavage intersection lineations generally parallel adjacent mesoscopic fold axes.

Locally, especially in some fold-hinge zones, the planar fabric gives way to a linear fabric (pencil structure) also sub-parallel to local fold axes. The occurrence of planar and linear fabrics in different parts of the

folds, the possible origin and the relationships of these fabrics with structural position have been discussed in MAZZOLI & CARNEMOLLA (1993).

In the competent beds, a centimetrically spaced cleavage is observed mainly in the zones of high strains, e.g. in close proximity to thrust contacts or in the hinge zone of tight folds (Fig. 14). Pressure solution surfaces defining thin sutured cleavage domains are very common in competent beds (Fig. 15) and are best observed in thin section (MAZZOLI, 1993b).

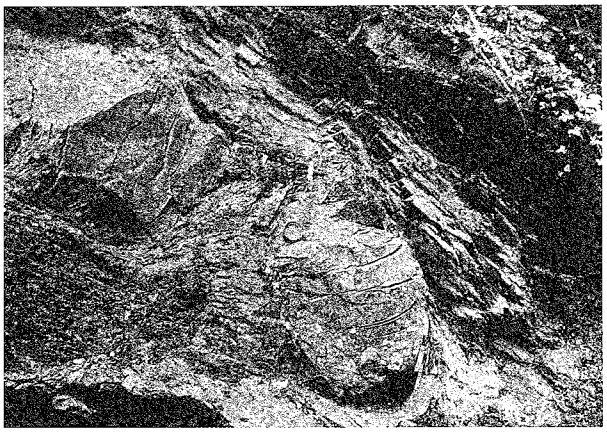

Fig. 14 - Hinge zone of gently inclined, tight synclinal fold in Lower Cretaceous "Galestri" NE of Varcovalle (E is to the left). Note convergent spaced disjunctive cleavage in the competent limestone bed and divergent slaty cleavage in the argillites.

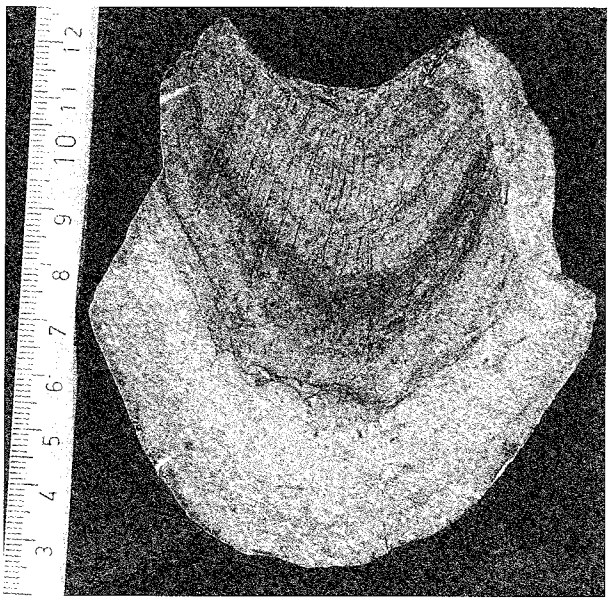

Fig. 15 - Polished surface of hinge zone of metric parasitic fold from the uppermost "Calcari con selce" SW of M. Papa. Note thin sutured cleavage domains in the inner arc and roughly radial calcite extension veins in the outer arc. These structures are indicative of a buckling origin of the fold, with deformation of the competent layer mainly accommodated by tangential longitudinal strain.

*Major folds and thrusts.* - Internal deformation of the Lagonegro Unit I can be best observed in the M. Sirino group due to the strong vertical relief (Fig. 16a & b). In profile B-B'' of Fig. 4, a gradual transition can be observed from upright folds to the west (Mad. di Sirino), to steeply and then moderately inclined structures (M. Papa), to gently inclined folds to the east (Serra Orticosa). A gently-dipping thrust fault at the base of the eastern slope of the Sirino group brings the overturned limb of the Serra Orticosa anticline (consisting of "Calcari con selce") onto upright "Galestri" in the footwall. In this area the thrust shows its maximum displacement (of several hundreds of meters). The thrust is cut to the north by a later normal fault; however, to the south the thrust displacement can be observed to gradually decrease as the axial plane of the anticline in the hangingwall becomes steeper, until eventually the thrust dies out giving way along strike to an anticline-syncline pair (west of C' in profile C-C'', Fig. 4). A similar feature also occurs for the higher thrust fault shown (at B') in profile B-B'', which can be observed to die out into folds at both lateral tips. To the south, another thrust fault occurs which shows an en-echelon relationship to the previous one (Fig. 2).

*Discussion.* - Thrust faults are often observed to die out into folds at their lateral tips (e.g. COWARD & POTTS, 1983). This feature has been related to thrust propagation into already folded rocks (e.g. ELLIOTT, 1976; COWARD & KIM, 1981; FISCHER & COWARD, 1982; COOPER & TRAYNER, 1986). According to these authors, a ductile bead of deformation would develop ahead of - and would be faulted by - a propagating smooth-trajectory thrust. A model for thrust-related folds which evolved from an initial stage of sinusoidal buckling has also been recently proposed by FISCHER *et alii* (1992). These models are opposed to the traditional models of staircase-trajectory thrust (e.g. RICH, 1934; BOYER & ELLIOTT, 1982; SUPPE, 1983) or flat lying detachment (JAMISON, 1987), in which the thrust propagates into undeformed rocks and the result of thrust sheet motion is to produce rootless hangingwall anticlines. Ideal detachment and staircase-trajectory thrusts should preserve an undeformed footwall, while hangingwall rocks should record only those strains due to the formation of the rootless anticline which depend largely on the preferred mechanism of folding. To differentiate between the cases of thrusts propagating into essentially undeformed rocks and smooth-trajectory thrusts propagating into already folded rocks, two main criteria are considered in the present study.

(1) *Fold origin.* Two main groups of folds may be used to explain the kinematics of thrust-related folding: kink-like hangingwall folds and buckle folds. Three geometric types of thrust-related kink-like hangingwall folds are generally recognized in foreland fold and thrust belts: ramp-flat folds, detachment folds and tip-line folds. Ramp-flat folds result from stratigraphic duplication at a thrust ramp where hangingwall ramps overlie footwall flats (RICH, 1934). Detachment folds commonly develop above a detachment that is subparallel to bedding and are cored by incompetent, often disharmonically folded strata (DAHLSTROM, 1970; LAUBSCHER, 1976). Tip-line folds develop as a result of enhanced compression and shortening above, or in front of, the tip line of a blind thrust (ELLIOTT, 1976). Ramp-flat folds do not form at blind thrust tips and therefore cannot be tip-line folds. In contrast, detach-

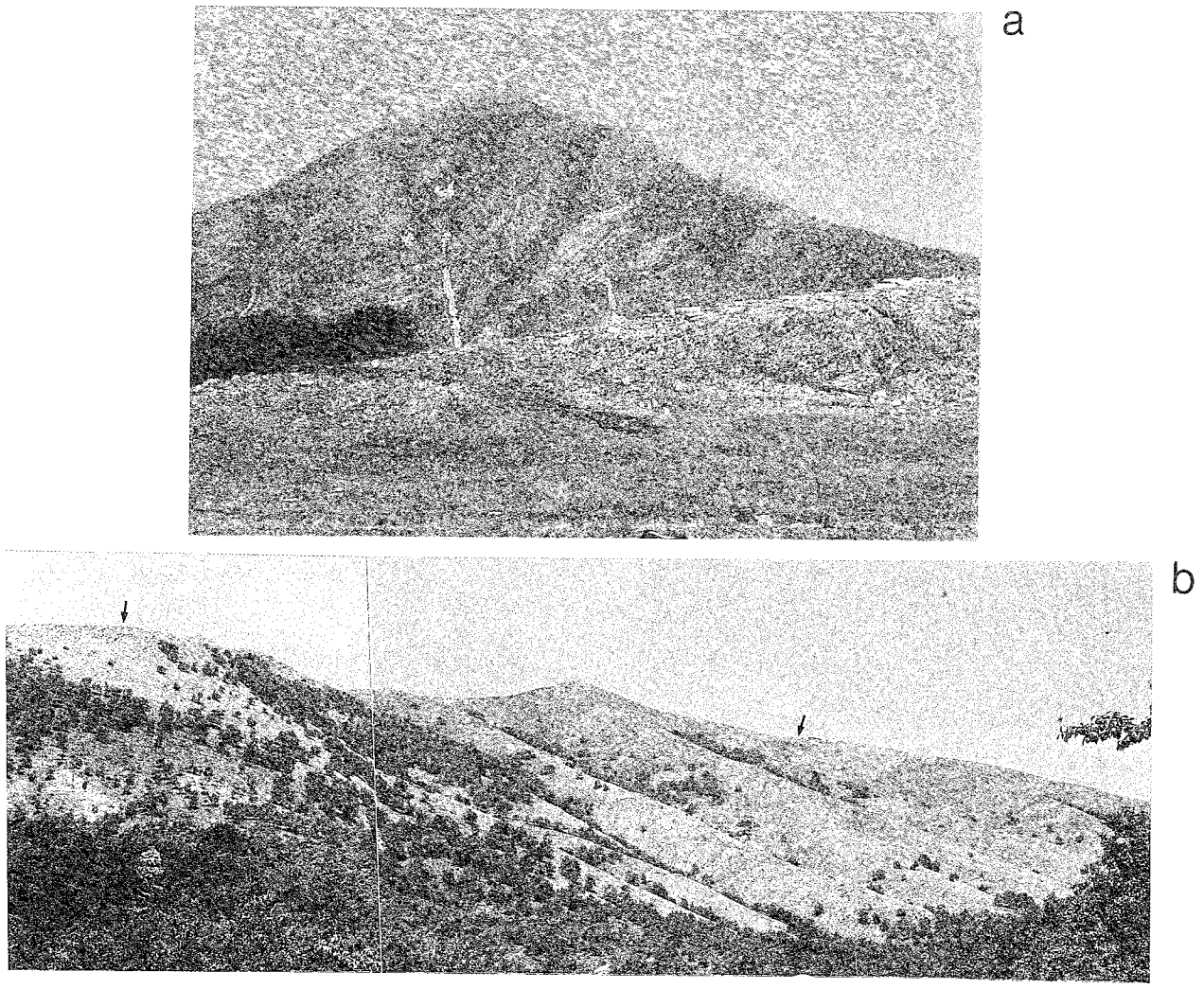


Fig. 16 - Structural features of Lagonegro Unit I, M. Sirino group (E is to the right of the pictures). (a) View of the southeastern slope of M. Papa (background) showing moderately inclined NE-verging tight folds (vertical relief is about 400 m). The area corresponds to that in the hangingwall of the thrust shown at B' in profile B-B'' (Fig. 4). Jurassic cherts (''Scisti silicei'') in the foreground belong to the footwall. (b) Eastern slope of M. Sirino group. Note gently inclined chevron folds in the ''Calcari con selce'' on upper left (Serra Orticosa) and overturned Jurassic cherts below (white). Folds along the slope to the right correspond to those shown in the eastern part of the profile B-B''.

ment folds may form at the tip line of a thrust that is sub-parallel to bedding and therefore may be tip-line folds (JAMISON, 1987). Asymmetric, open to close, often overturned thrust-related folds that verge toward the foreland are commonly suggested to have formed as tip-line folds (FISCHER *et alii*, 1992 and references therein). The kinematics of formation of these folds has been explained using fault-propagation fold (e.g. SUPPE, 1985) or detachment fold (JAMISON, 1987) models (Fig. 17a & b). In all these models, folding is essentially a passive process occurring in the hangingwall of a thrust surface. Fold geometry is a function of fault shape and displacement in the cases of ramp-flat folds and fault-propagation folds (e.g. SUPPE, 1983, 1985), while fold amplitude is related to the thickness of a basal detachment layer in the case of detachment folds. These models assume that structures evolve passively as migrating-hinge kink folds deformed only by slip on bedding planes between fold hinges, and imply that cumulative strain is constant and homogeneously distributed in the fold limbs. The problems related to such passive kink-like thrust-related folding models have been discussed by RAMSAY (1992) who also emphasized, based on the original work of Heim in the Helvetic nappes, that thrust surfaces may develop in some cases as a secondary feature of folds as the result of the shearing out of the middle limbs of antiform-synform pairs.

In the present case, pervasive folding at different scales is observed both in the hangingwall and in the footwall of thrust faults (Figs. 16 & 18). Analysis of the thickness variations of the competent and incompetent beds, small-scale structures and the cleavage pattern (i.e. finite strain trajectories) in beds of differing competence all indicate an origin of the folds by buckling mechanisms (Figs. 14, 18b & c). The overall cuspate-lobate geometry shown by major folds (Fig. 2), with tight, sharp hinged (''pinched'') synclines of ''Galestri'' and radiolarian cherts between broader anticlines of competent ''Calcari con selce'' also suggests that layers were mechanically active during folding. This is in contrast with the idea of passive fold development implied by fault-bend, fault-propagation or detachment fold models. However, although single folds have a buckling origin, the large-scale structural

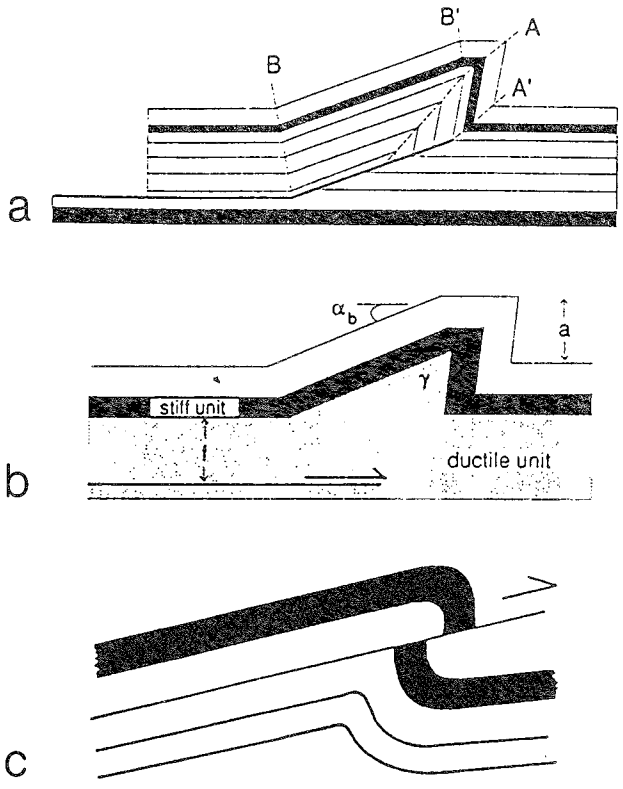


Fig. 17 - Thrust-related fold models (a & b from FISCHER *et alii*, 1992). (a) Staircase-trajectory thrust with fault-propagation fold. (b) Flat-lying thrust with detachment fold. (c) Smooth-trajectory thrust cutting through previously folded beds (after COOPER & TRAYNER, 1986).

geometry may have been modified by transport of the thrust sheet over an irregular ramp-flat morphology in its underlying thrust surface. For instance, the large anticlinorium defined by the Upper Triassic limestones in profile B-B'' (Fig. 2) could result from an overall upward deflection of the hangingwall due to movement above a ramp in the thrust surface at the base. Evidence for this is provided by the progressive shallowing of the axial surfaces and fold tightening towards the front of the thrust sheets. These features closely resemble the geometry shown by RAMSAY (1989) for buckle folds developed above irregular ramp-flat thrust surfaces as the result of shear strains within the sheets (Fig. 19).

(2) *Footwall deformation*. In its footwall, an ideal staircase-trajectory thrust should show no fabric or strain developed during its propagation and the staircase geometry should be preserved; the beds in the footwall should be planar and unfolded. In the case of an ideal smooth-trajectory thrust (Fig. 17c), the footwall should display strain and/or fabrics developed prior to and during thrust propagation. In the present case, the footwall of the thrusts is usually highly strained, showing pervasive tight folding and cleavage fabrics (Fig. 20a & b). Furthermore, minor reverse fault planes associated with the thrusts can be observed to clearly postdate fold formation in the footwall.

On the basis of the foregoing considerations, the structural evolution for the Lagonegro Unit I during the main ($D_1$) deformation sequence may be envisaged as follows:

(1) Buckling of the multilayer succession occurs with the M. Facito Fm. acting as the main décollement level. First-order wavelength during buckling is mainly controlled by the 500 m-thick competent limestones of the "Calcari con selce" which represent the mechanically dominant member in the succession. The M. Facito Fm. mostly consists of several hundreds of meters of shales (Fig. 3), representing a thick incompetent level at the base of the multilayer. Moreover, the up to several kilometers large neritic limestone blocks observed within this formation in the upper Lagonegro nappe - interpreted as olistoliths derived from the progressive collapse, during Middle Triassic rifting, of a pre-existing carbonate platform (WOOD, 1981) - are likely to be absent in the more distal sediments of Unit I.

(2) Smooth-trajectory thrust faults propagate into the already deformed multylayer cutting through steep/inverted fold limbs ("break thrusts").

(3) Fold geometry is modified by the shear strains due to the riding of thrust sheets over irregular thrust surfaces with ramp-flat footwall topography.

## ORIENTATION ANALYSIS FOR LAGONEGRO UNIT I

Although most of the early ($F_1$) fold structures are sub-horizontal to moderately plunging, a strong variability is displayed by fold axial traces and axial trends within the whole study area (cf. geological map). As an example, $F_1$ fold axis azimuths from the central part of the M. Sirino group are shown in Fig. 21, using both minor fold hinges and the strike of vertical beds. Orientations lie in the whole range of angles from NW-SE to NE-SW, and appear not to be related to different thrust sheets. In fact, structurally homogeneous domains include parts of different thrust sheets (Fig. 21). The change in structural orientation may appear to be quite abrupt, as for example between the NW-SE-oriented folds of M. Papa and the area to the northeast, where a large NE-SW-trending anticline is observed (Fig. 22). However, where rock outcrop is more continuous, the orientation of structural elements can be observed to change progressively, defining arcuate features with lengths of several hundreds of meters to two kilometers at most. For instance, structural trends in the area of Mad. di Sirino can be observed gradually changing orientation from NW-SE to NE-SW within a few hundreds of meters, moving from north to south (Fig. 23). Due to their limited dimensions and to the absence of a direct relationship to the thrusts, these arcuate geometries appear not to be primary - i.e. thrust-related - features. They are interpreted to result from later ($D_2$-related) distortion of originally less arcuate and more continuous structures, as will be discussed below. Extreme variability of early fold orientations is observed in the southern sector of Fig. 21 (La Coddatella). This variability results from pervasive $D_2$ deformation in this area, shown by numerous roughly E-W oriented $F_2$ folds (Fig. 24).

## STRUCTURAL ELEMENTS OF THE $D_2$ DEFORMATION PHASE

Outcrop-scale structures related to this deformation phase are discontinuously developed in all the lithologies, but are more common in rock units comprising alternations of competent and incompetent

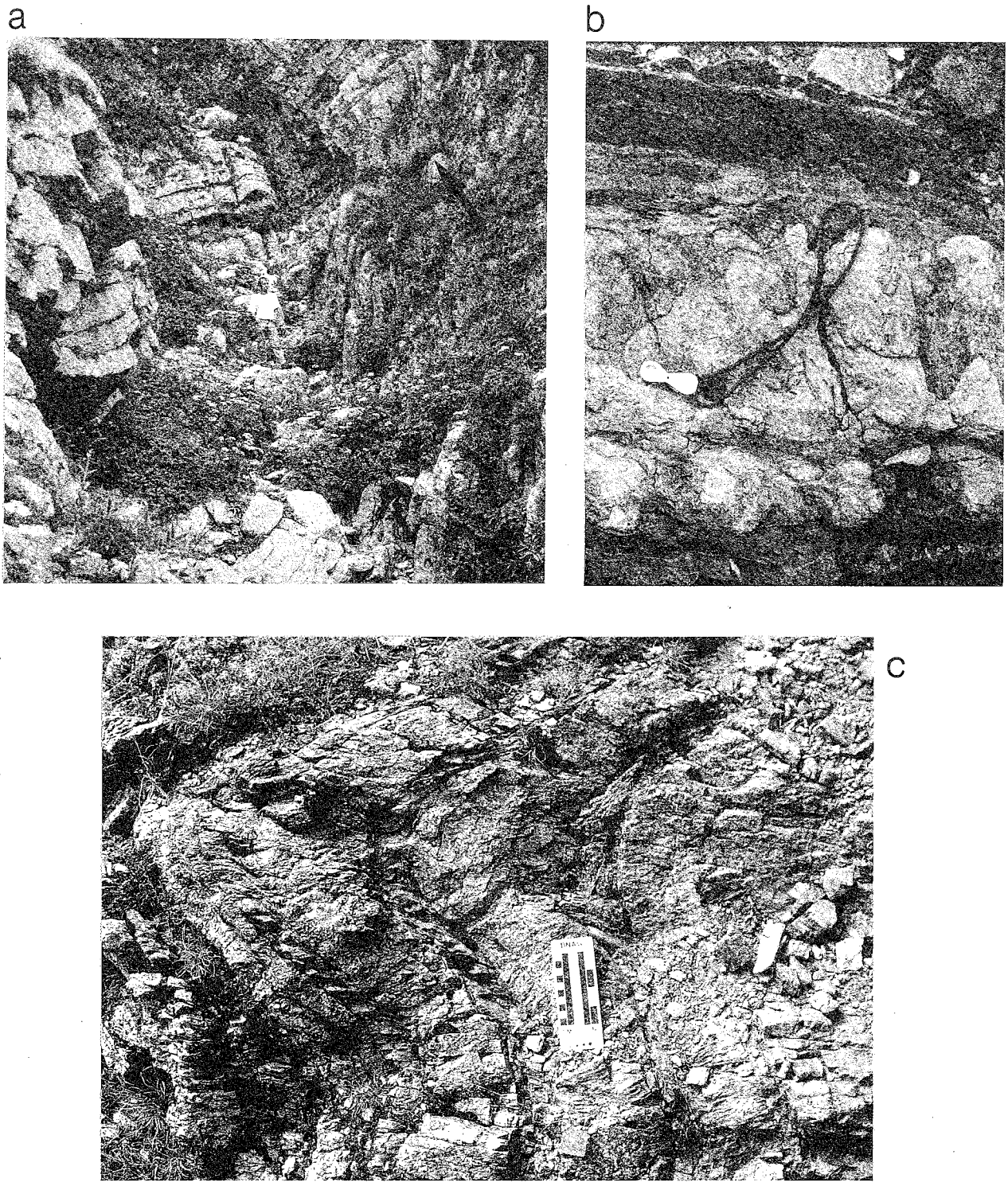


Fig. 18 - Minor fold structures in Lagonegro unit I. (a) Tight anticlinal fold (hinge on the upper right) in "Calcari con selce" SE of Mad. di Sirino (E is to the right). (b) Cuspate-lobate folds in interbedded cherts, calcilutites with chert nodules and argillites, upper part of the "Calcari con selce" SE of Mad. di Sirino. (c) Recumbent folds in radiolarian cherts ("Scisti silicei") NE of Varcovalle (E is to the left). Note parallel fold geometry and convergent cleavage fan in more competent layers, and class 3 fold geometry associated with divergent cleavage in less competent layers.

Fig. 19 - Schematic diagram to illustrate fold geometry resulting from shear strains within a thrust sheet moving above an irregular ramp-flat thrust surface (from RAMSAY, 1989).

beds, such as the "Galestri" and the argillite-rich member in the lower part of the "Calcari con selce". The structures related to this deformation fold both bedding and slaty cleavage associated with the principal period of deformation found in these rocks (Fig. 25).

Mesoscopic $F_2$ folds in competent limestone beds of the "Galestri" have wavelengths of several cen-

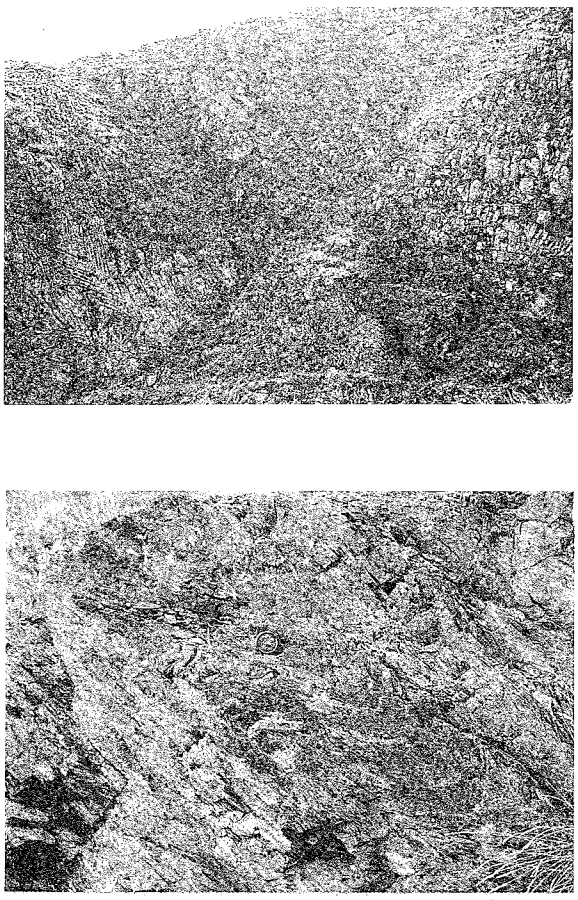


Fig. 20 - Thrust fault about 1 km ESE of M. del Papa (east is to the left). Location is approximately B' in profile B-B'' (Fig. 4). (a) Upper Triassic ''Calcari con selce'' in the hangingwall belong to the normal limb of a syncline; Jurassic cherts (''Scisti silicei'') in the footwall belong to the inverted limb of a syncline (note *z*-shaped chevron folds). (b) Tight folds and well-developed axial plane cleavage in overturned argillites in the footwall (basal part of the ''Scisti silicei'').

timeters to 2.5 m and amplitudes from few centimeters to 1.5 m. They are mostly symmetric, open to tight, with rounded hinge zones (Fig. 25a & b). Fold plunges vary depending on structural position relative to early ($F_1$) folds; however, most of the $F_2$ are sub-horizontal to moderately plunging (Fig. 26a). This feature reflects field outcrop frequency: $F_2$ folds superposed on shallow dipping normal limbs of $F_1$ structures are exposed over much larger areas than those developed on steep/inverted limbs of early folds (Fig. 27). This bias on the sampling probably contributes to the consistency of axial directions measured over the whole study area (Fig. 26a). The stability of axial directions of second phase folds is probably also enhanced by the high angle between the axial surface of $F_2$ and the surfaces being folded (RAMSAY, 1967).

The wavelength of mesoscopic $F_2$ folds developed in $S_1$ slaty cleavage is controlled by the wavelength of adjacent buckled competent layers. Due to their cross cutting relationships, bedding and early cleavage are expected to undergo refolding in different axial orientations (RAMSAY & HUBER, 1987). In the studied rocks, however, axial orientations of both meso- and microscopic folds developed in slaty cleavage (Fig. 26b & c) are similar to those developed in refolded competent beds (Fig. 26a). This feature is probably related to the generally small angle between cleavage and bedding (MAZZOLI & CARNEMOLLA, 1993).

Centimetric to sub-millimetric folding of the early slaty cleavage fabric produces heterogeneous crenulation cleavages ($S_2$) discontinuously developed in the argillites (Fig. 25c & d). Where crenulation cleavage is more intensely developed, attaining a discrete character, the rock may be easily split in the directions of the fissile surfaces defined by $S_1$ and $S_2$ and a pencil fabric develops. The orientation of such pencils is generally sub-parallel to $F_2$ axes measured in adjacent folded competent beds.

A single non-conjugate set of crenulation cleavage planes, approximately parallel to the axial surfaces of adjacent $F_2$ folds in competent beds, is occasionally observed (Fig. 28). In most of the cases, however, an $S_2$ fabric is developed in these rocks in the form of crossing conjugate cleavage planes (Fig. 25d). Conjugate cleavages have different attitudes depending on the orientation of the early slaty cleavage fabric (which varies from sub-horizontal to sub-vertical). They always show contractional kink band geometries, recording local layer parallel shortening of the early fabric. Kink bands have widths from few tens of microns to few centimeters and lengths of up to more than 1 m; they commonly terminate abruptly against bedding surfaces of adjacent competent layers. The angle between the two differently oriented kink band arrays which faces the inferred shortening direction is invariably obtuse, varying from 126° to 159° (mean dihedral angle is 142°). Conjugate kink folds vary from symmetric to asymmetric. Comparison with experimental work suggests that symmetric conjugate folds arise when the principal compressive stress is aligned parallel to the folded planar fabric, while asymmetric relationships develop when this stress direction is obliquely inclined to the early fabric (e.g. RAMSAY & HUBER, 1987). In the majority of the outcrops analysed, both sets of kink bands are observed. Although in some cases conjugate kinks show different degrees of development with one set being dominant over the other, it is only rarely that one set of kinks alone is developed. According to RAMSAY & HUBER (1987) this feature would suggest that in most of the cases the principal directions of the overall ($D_2$-related) bulk strain were close to parallel and perpendicular to the general trend of the early fabric. It must be noted, however, that the effect of stress refraction due to anisotropy could lead to the development of conjugate structures even when such conditions of sub-parallelism and sub-perpendicularity do not occur (COBBOLD, 1976).

In thin section, $S_2$ cleavages consist of small symmetric to asymmetric crenulations folding a continuous cleavage defined by very fine grained phyllosilicates and clastic grains (Fig. 29). Both discrete and zonal crenulation cleavage types of GRAY (1977a) are developed. Discrete crenulation cleavages are thin, dark planar discontinuities which have sharp distinct boundaries that truncate the crenulated preexisting fabric; zonal crenulation cleavages are laminar domains rich in phyllosilicates, coincident with differentiated limbs of microfolds. The two cleavage types may be observed progressivly grading into one another and into undifferentiated microfold limbs, confirming that they represent different stages in the process of crenulation

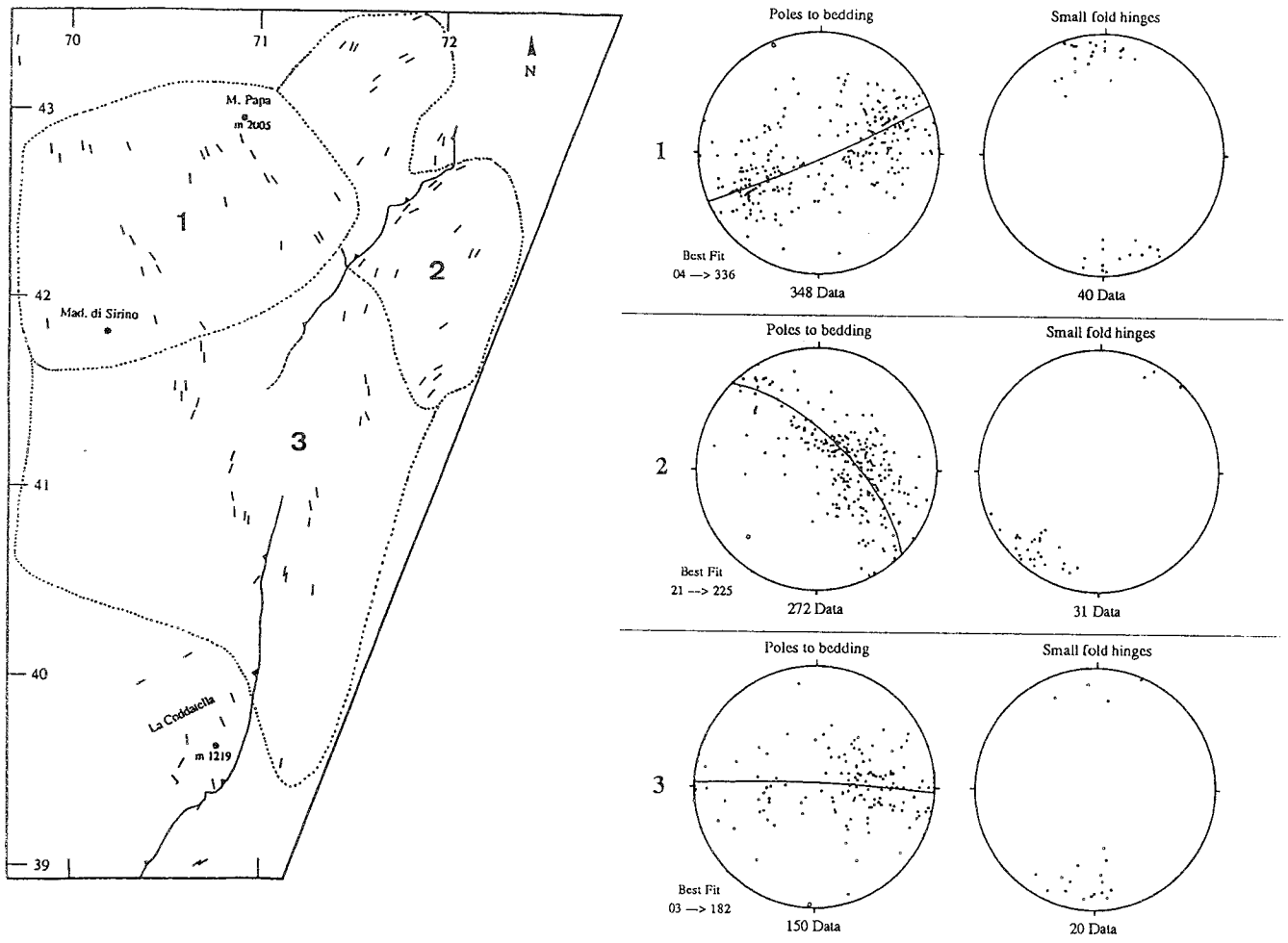


Fig. 21 - Azimuths of $F_1$ fold axes determined from minor $F_1$ fold hinges and strike of vertical beds in the central area of the M. Sirino group (kilometric grid of the "Foglio 210 della Carta d'Italia" is shown). Orientation data from the three domains defined in the area also shown.

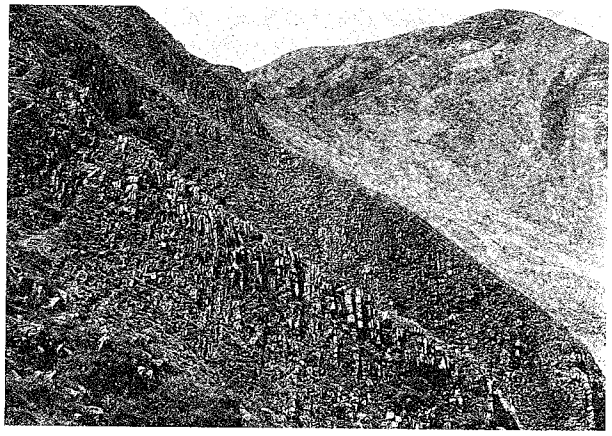

Fig. 22 - View of the SE-verging anticline NE of M. Papa. Sub-vertical SE limb in the foreground, shallow dipping NW limb in the background right (note chair lift for scale).

cleavage development (e.g. GRAY, 1979a). This mainly consists in the progressive tightening of buckle microfolds followed by differentiation by solution-transfer: the most soluble minerals (quartz, calcite) are removed from the limbs of "locked up" microfolds and reprecipitated in the hinge zones (e.g. GRAY & DURNEY, 1979).

From SEM observations, the conjugate structures are defined by the axial planes of conjugate kink folds in the undifferentiated fabric domains, or by more discrete domains of preferentially oriented phyllosilicates derived from the rotation and differentiation of microfold limbs (Fig. 30a-d).

Crenulation cleavage is only rarely developed as true crossing conjugate sets as it is observed here (e.g. COSGROVE, 1976; RAMSAY & HUBER, 1987). Based on the comparison with theoretical and experimental work on internal buckling within a confined anisotropic medium, Gray (1979b) suggested that the development of single or crossing conjugate axial planes depends on the parameter $\xi = L/2H$, where L = microfold wavelength and H = confinement distance (that is the thickness of the layer in which the microfolds are developed). Experimental data show that small values of $\xi$ favour single parallel sets developed approximately normal to loading, while conjugate sets oblique to the loading direction may arise if $\xi$ is appreciable. In the study area, the majority of the crenulation folds analysed have conjugate axial plane cleavages. In terms of frequency of occurrence, single parallel sets are scarce. This indicates that the wavelenghts of these natural crenulations, which are dependent on the fabric parameters (GRAY, 1977b), are comparatevely large with respect to the thickness of the layers in which they are developed.

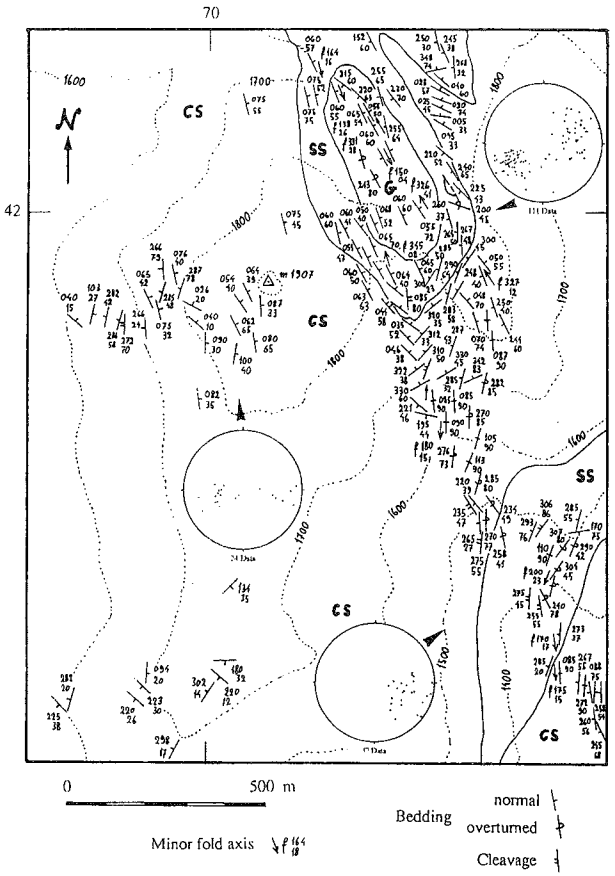


Fig. 23 - Geological map and orientation data (poles to bedding) for the area of Mad. di Sirino. CS = Calcari con selce, Upper Triassic; SS = Scisti silicei, Jurassic; G = Galestri, Lower Cretaceous. Kilometric grid of the "Foglio 210 della Carta d'Italia" is shown.

*$D_2$-related strains*

The geometry and orientation of conjugate folds and kink bands is often used to determine the directions of principal stresses acting during the formation of these structures (e.g. RAMSAY, 1962; RAMSAY & HUBER, 1987). However, as folds represent states of heteogeneous strain in anistropic rocks, they provide information about directions of principal strains and not stresses (e.g. RAMSAY, 1967; PATERSON, 1989). Stresses could have been variable during fold development as, in general, stress and strain axes do not maintain parallelism in anisotropic rocks (e.g. COBBOLD, 1976). Therefore, the geometrical relationships of conjugate structures are used in this study to infer directions of principal strain axes ($X \geq Y \geq Z$). By reinterpretaton of the "conjugate bisector" method of RAMSAY (1962), the intermediate strain axis (Y) is approximately parallel to the intersection of conjugate kink planes and the maximum and minimum strains bisect the kink planes (Fig. 31). According to STUBLEY (1990) the accuracy of the orientations determined by this method is probably of $\pm 20°$, based on the comparison with experimental results.

Orientations of the minimum strain axis (Z) calculated by the conjugate bisector method are plotted in Fig. 32a, while areal distribution of the data is shown in Fig. 32b. Mean shortening direction obtained by the analysis plunges 20° towards 198° and shows a general good agreement with the orientation of associated fold structures (Fig. 26).

Minimum estimates of $D_2$-related shortening were obtained from seven different localities by the analysis of competent layer folds. Single layer buckles

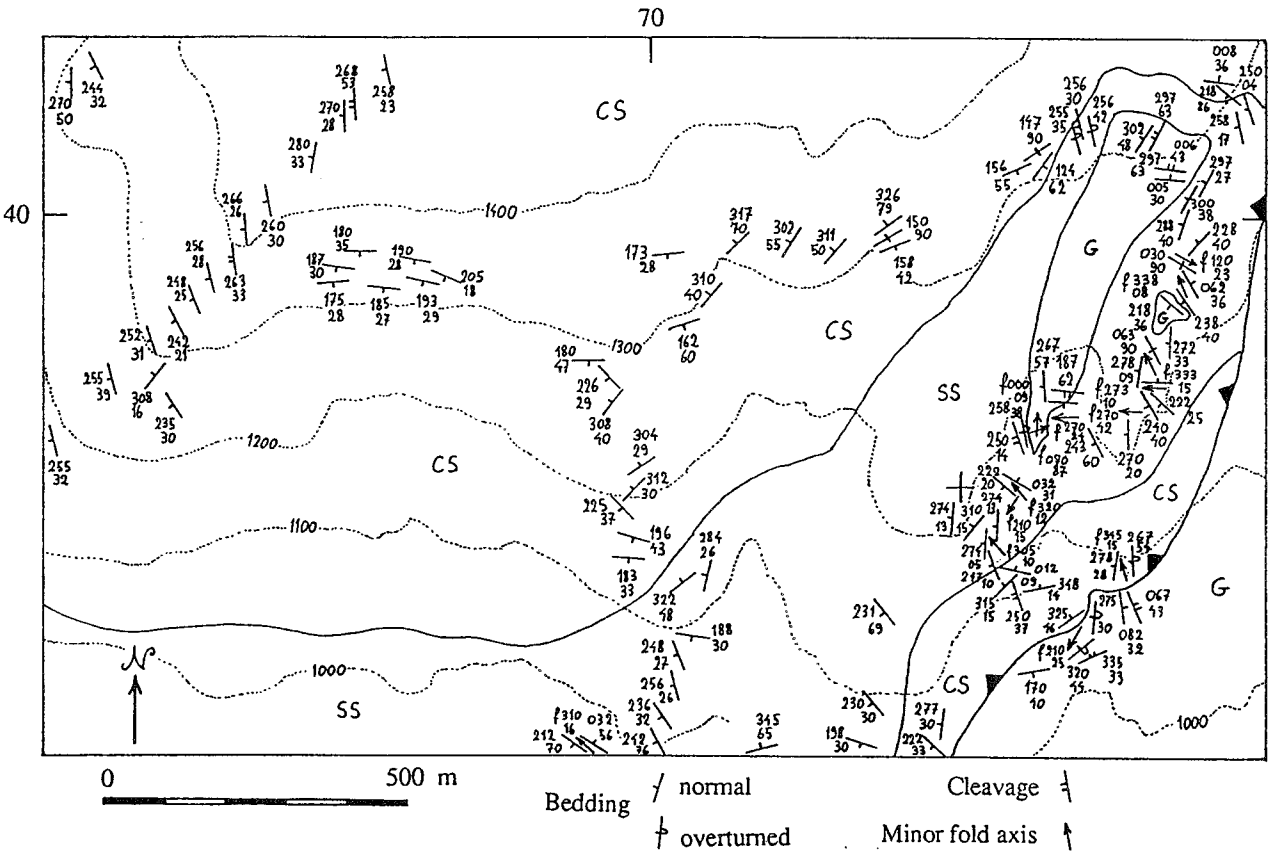


Fig. 24 - Geological map of the area of La Coddatella. CS = Calcari con selce, Upper Triassic; SS = Scisti silicei, Jurassic; G = Galestri, Lower Cretaceous. Kilometric grid of the "Foglio 210 della Carta d'Italia" is shown.

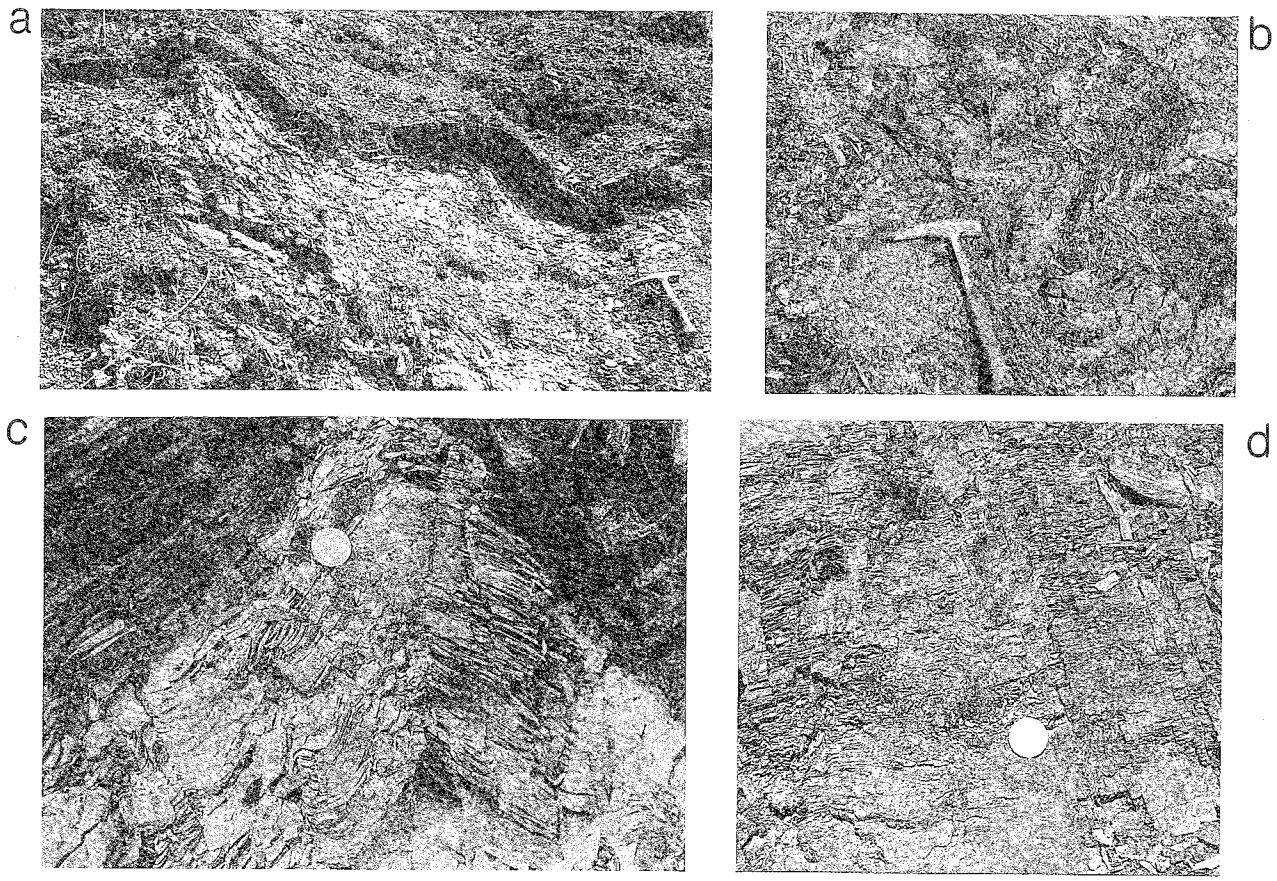


Fig. 25 - Mesoscopic $F_2$ folds in interbedded limestones and argillites of the Lower cretaceous "Galestri". (a) Open steeply inclined folds NE of Serra Orticosa. (b) Close to tight moderately inclined folds S of M. Papa. (c) Folded slaty cleavage at Il Gavitone. Note conjugate sets of crenulation cleavages. (d) Crenulation cleavages forming conjugate kink bands in the argillites E of Serra Orticosa.

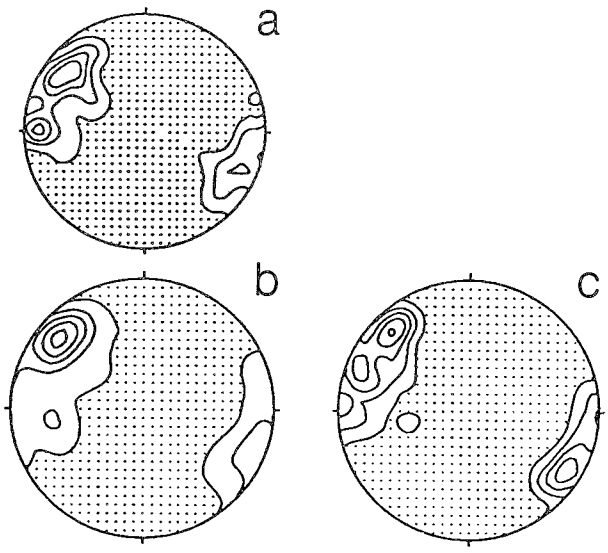


Fig. 26 - Orientation data for $F_2$ folds (whole study area). Contoured at 1, 3, 5... times uniform distribution. (a) Mesoscopic fold hinges in bedding (186 data). (b) Mesoscopic fold hinges in folded $S_1$ (36 data). (c) $S_1$-$S_2$ intersection lineations and microfold hinges (111 data).

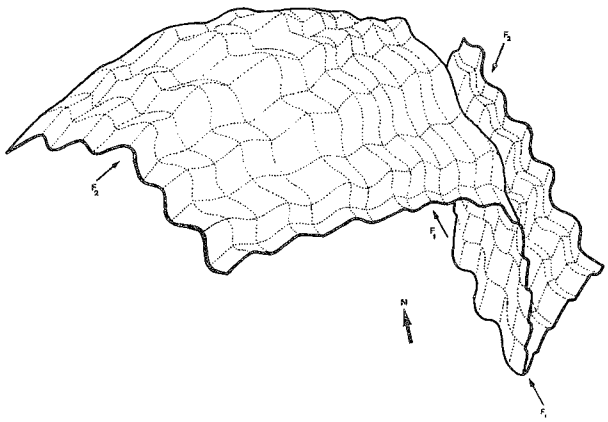

Fig. 27 - Schematic diagram of $F_1$-$F_2$ geometrical relationships. Note Type 1 interference patterns developed on earlier broad anticline and Type 2 patterns developed on earlier tight syncline. $F_2$ deamplification towards the early anticlinal crest is to show schematically the heterogeneous development of these folds.

(shown by disharmonic folding of adjacent competent layers) were used. The ptygmatic shape of folded competent layers (Fig. 25a & b) suggests a considerable competence contrast and implies a small amount of layer parallel shortening (e.g. RAMSAY & HUBER, 1987). In this situation, the comparison between the arc length of the central line of the competent layer and the length of the median surface of the fold wave can be used to

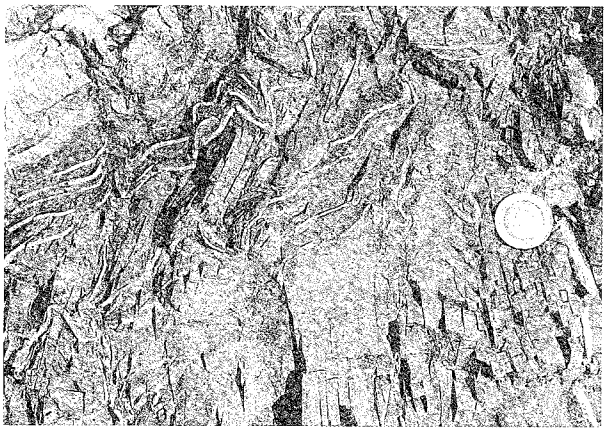

Fig. 28 - Buckled bedding-parallel calcite veins in the inner arc of $F_2$ fold in interbedded limestones and argillites ("Calcari con selce" E of M. Niella). Note crenulation cleavage (developed in a single parallel set axial planar to $F_2$).

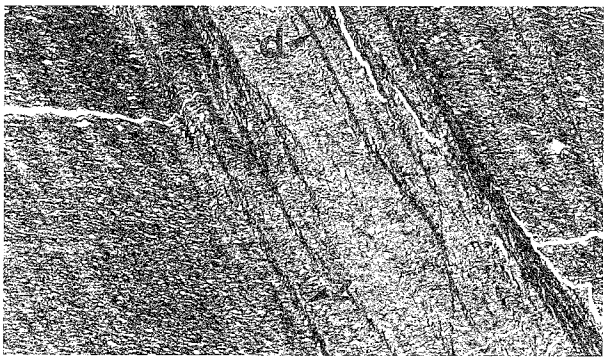


Fig. 29 - Microphotograph of thin section showing one of two conjugate crenulations deforming pre-existing slaty cleavage (roughly horizontal). Note discrete (*d*) and zonal crenulation (*z*) cleavages, and crenulation microfolds. Picture is 3.4 mm across.

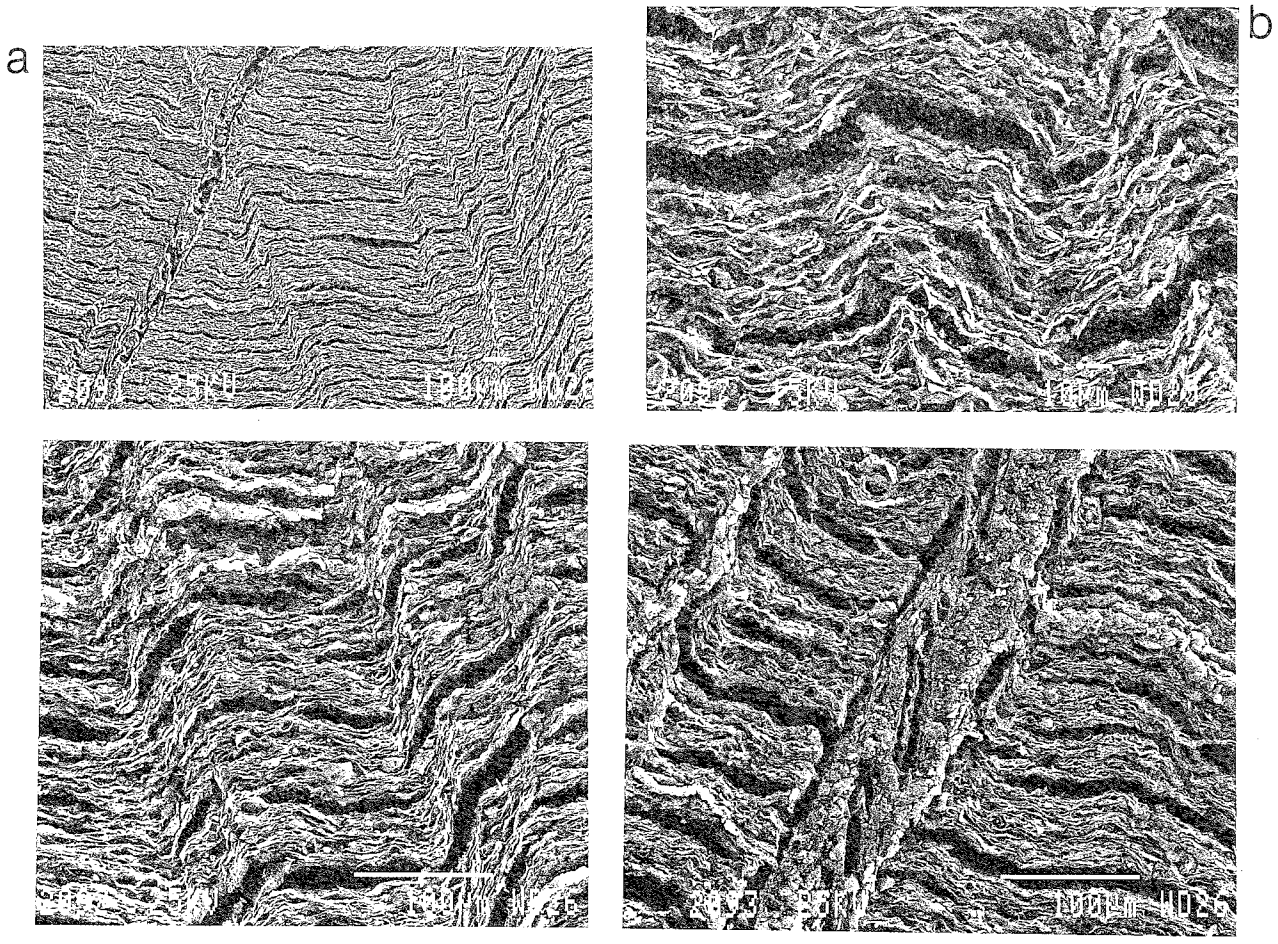


Fig. 30 - (a) SEM photograph of polished surface showing conjugate microfolds and crenulation cleavages deforming early slaty cleavage fabric (roughly horizontal). (b) Detail of (a) showing symmetric conjugate kink folds. (c) Detail of (a) showing incipient zonal cleavage development along steeply dipping narrow fold limbs. (d) Detail of (a) showing zonal cleavage formed by the reorientation of phyllosilicates along a former fold limb.

estimate minimum amounts of shortening. Values determined by this method range from 1% to 52% (mean 28%). Considering the heterogeneous character and the discontinuous development of $D_2$ structures, however, it is difficult to assess an average amount of shortening on the regional scale.

## TIMING OF THE DEFORMATIONS

The onset of thrusting leading to the emplacement of Lagonegro Unit II onto Lagonegro Unit I cannot be directly dated, as the youngest sediments on top of the lower nappe in the study area are Lower Cretaceous

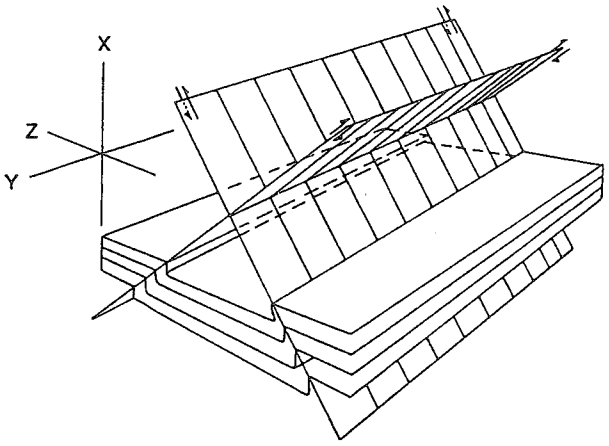


Fig. 31 - Schematic diagram of conjugate kinks and relationship to the strain ellipsoid axes $X \geq Y \geq Z$ (from RAMSAY, 1962, modified after PATERSON, 1989).

tonian-Messinian) for the onset of deformation within the Mesozoic Lagonegro units; this deformation was preceded by the detachment of the Tertiary sedimentary covers from their Mesozoic substratum (LENTINI *et alii* 1990; ROURE *et alii*, 1991).

For the same reason as above (the youngest Lagonegro basin sediments within the study area are of Lower Cretaceous age), also the later ($D_2$) shortening cannot be directly dated. Dominant N-S to NNE-SSW compression, thus with a similar orientation to the shortening determined from $D_2$-related structures in the study area, has been shown in the nearby Sant'Arcangelo basin and dated as Early-Middle Pliocene (HIPPOLITE *et alii*, 1991). However, it has to be noted that NNE-SSW shortening characterises the youngest (Early Pleistocene) structures throughout the whole southern sector (Campania-Lucania segment) of the southern Apennines (CINQUE *et alii*, in press).

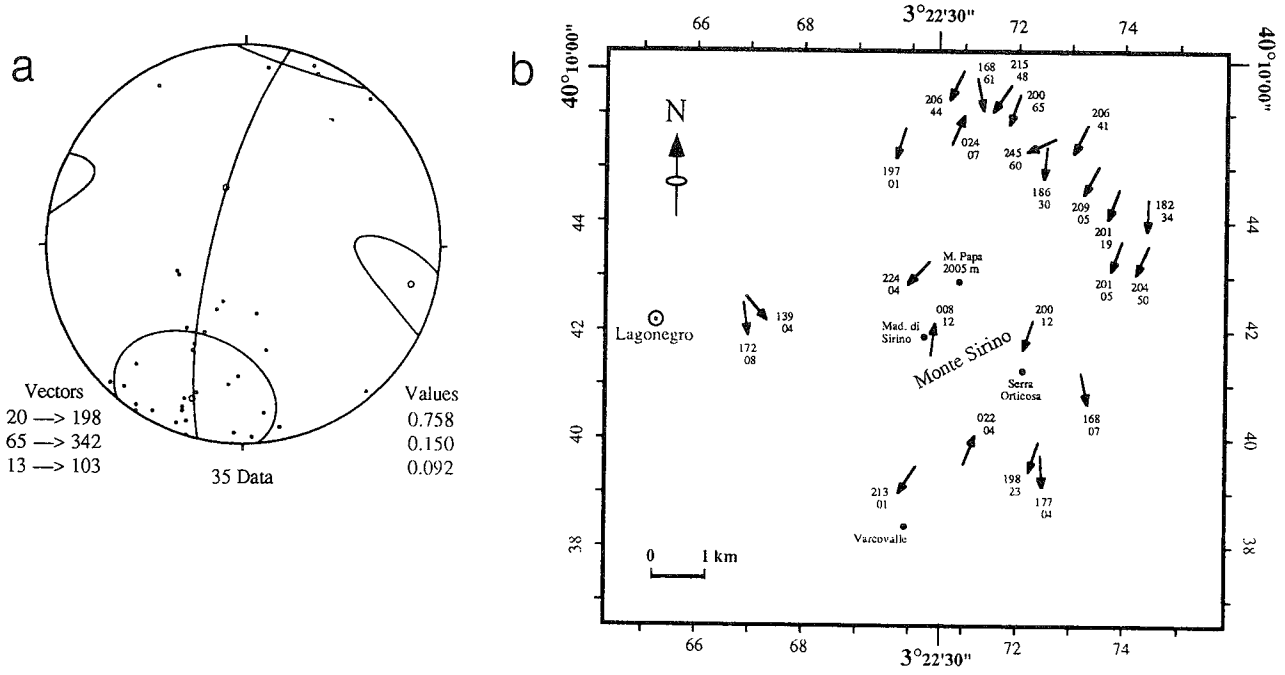


Fig. 32 - Orientation of maximum shortening axes from conjugate kink bands (conjugate bisector method). (a) Plotted data represent mean values from 35 locations around M. Sirino (mostly Lower Cretaceous argillites). The data were treated by Bingham statistics, giving the three eigenvectors which estimate the directions of the principal axes of symmetry of the parent population. The mean direction for the maximum shortening plunges 20° towards 198° (95% confidence cones are shown). (b) Areal data distribution.

in age and thrusting is certainly much younger. According to SCANDONE (1972, 1975b), deformation probably initiated in Langhian time based on the observation of Numidian Flysch on top of Lagonegro Unit II. A Langhian age is also suggested by MOSTARDINI & MERLINI (1986) and by HILL & HAYWARD (1988) based on section balancing of seismic reflection profiles across the whole chain and of geological cross sections calibrated by well data. CASERO *et alii* (1988) indicate a similar age for the initiation of thrusting in the internal part of the basin. However, recent geodynamic reconstruction suggest a younger age (i.e. Upper Tor-

## INTERFERENCE PATTERNS

Different types of the interference patterns defined by RAMSAY (1967) developed in the study area as a result of fold superposition. Transitional forms between Type 1 and Type 2 interference patterns are most commonly observed, indicating that later shortening was sub-parallel or at a small angle to early fold hinges. True (end member) Type 1 or Type 2 patterns are never observed, as fold superposition in this area produced mostly transitional forms between the two. For this reason, the structural descriptions below refer to "dominant interference patterns".

*Dominant Type 1 interference patterns.* Throughout the Lagonegro - M. Sirino area several dome-shaped structures can be seen (cf. geological map). M. Sirino itself represents a large dome-like structure, complicated by further interference structures on a smaller scale in its interior. The large dome is bounded by steep normal faults on its northern and northeastern sides, but in its southern sector the southern plunge of the structure can be clearly observed (Figs. 24 & 33). Around M. Sirino, several broad anticlines show a dome-like shape. Some, like those of M. Gurmara and M. Castagnareto (Fig. 34) are short and nearly circular. Others, like those of M. Milego and Bramafarina, although showing closed outcrop patterns, have a more elongated shape (Fig. 2). These structures are also sometimes partially fault-bounded. This feature is probably due to the fact that the behavior of the rock units during superposed deformations at very low-grade metamorphic conditions (MAZZOLI, 1993b) was not completely ductile. Partially fault-bounded interference structures similar to those mapped at Lagonegro have been described by DE SITTER (1952) in non-metamorphic Mesozoic sediments in the Atlas Mountains of Morocco. According to RAMSAY (1967), in non-metamorphic terranes the adaption of curvature of the sedimentary beds into the interference forms may lead to the setting up of a complex stress system in the layers and to the brittle fracture of the rocks in a complex series of faults. Recently LISLE *et alii* (1990) showed how, during refolding, consistent geometrical problems arise in the accommodation of curvature of competent layers if high competence contrasts occur in the sequence.

Outcrop-scale examples of dome and basin interfence structures are seen at different localities from major dome-shaped structures (for instance, on top of M. Milego). They are best developed in the Jurassic radiolarian cherts (Fig. 35) but may be observed also in the cherty limestones (Fig. 36a & b).

*Dominant Type 2 interference patterns.* In this type of fold superposition, the axial surface and both limbs of the early folds are folded together. These interference structures are (at least in part) responsible for the arcuate patterns of $F_1$ hinges in map-view (Fig. 21). They mainly affect tight, sharp hinged synclines, as in the case of Mad. di Sirino (Fig. 23), La Coddatella (Fig. 24), Il Gavitone (Figs. 37 & 38). Associated outcrop-scale structures consist of $F_2$ folds at a high angle to $F_1$ hinge orientation, showing variable plunge depending on their position relative to earlier structures (Fig. 39).

*Discussion.* - On the basis of the observations above, it appears that early fold shape is the major controlling factor on the type of interference pattern which developed in the study area. The axial surfaces of tight sharp hinged folds are folded, forming dominant Type 2 patterns of interference, whereas folds with larger interlimb angles and rounded hinges tend to develop Type 1 patterns. The

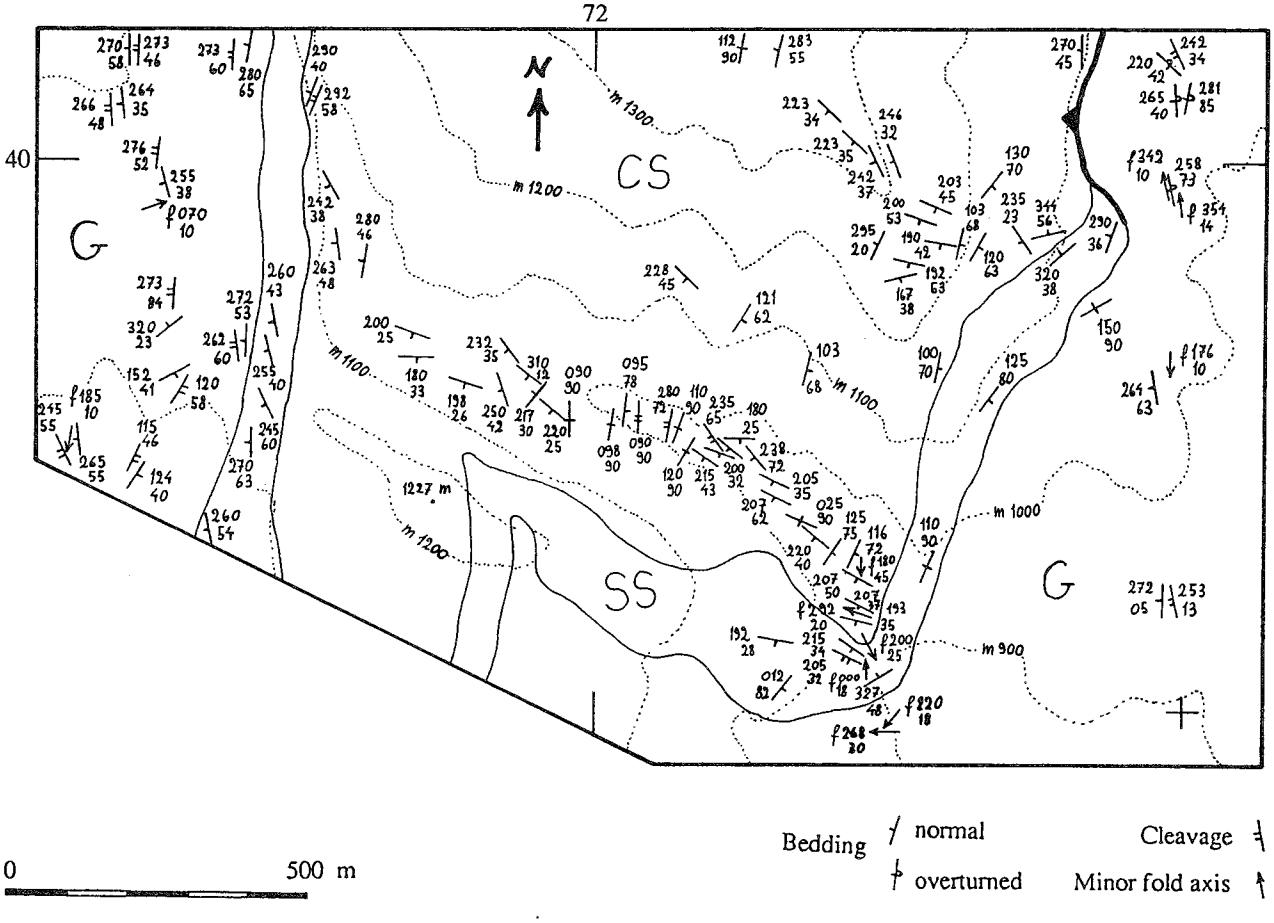


Fig. 33 - Geological map of the southern sector of Serra Orticosa. CS = Calcari con selce, Upper Triassic; SS = Scisti silicei, Jurassic; G = Galestri, Lower Cretaceous. Kilometric grid of the "Foglio 210 della Carta d'Italia" is shown.

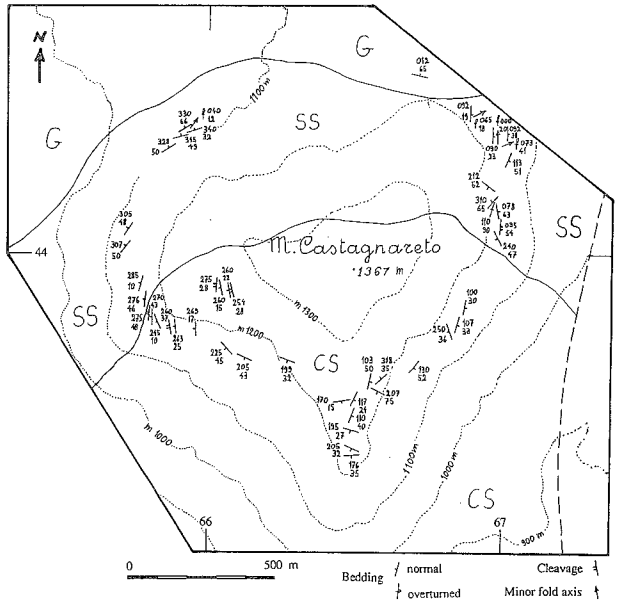


Fig. 34 - Geological map of M. Castagnareto dome. CS = Calcari con selce, Upper Triassic; SS = Scisti silicei, Jurassic; G = Galestri, Lower Cretaceous. Kilometric grid of the "Foglio 210 della Carta d'Italia" is shown.

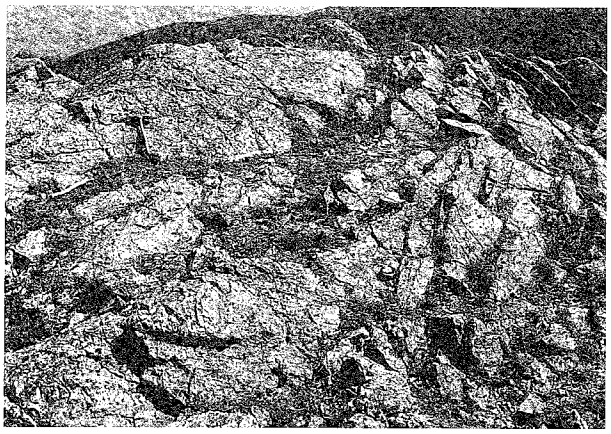

Fig. 35. Minor structure associated with dominant Type 1 fold superposition: dome-shaped anticline from the crest region of broad anticlinal fold NW of Mad. di Sirino (radiolarian cherts).

overall cuspate-lobate geometry of early folds, consisting of tight, sharp-hinged synclines between broader anticlines, results in a pattern of large domes surrounded by tight synclines showing arcuate axial trends (Fig. 27). This pattern is further complicated by the presence of thrust faults (predating $F_2$) and of the fold-bounding faults discussed above (cf. geological map).

Experimental analogue models of superposed buckling suggest that early fold geometry exerts a major influence on the patterns of interference (e.g. WATKINSON, 1981; GHOSH *et alii*, 1992). The parameters of the early folds which mostly affect the geometry of the superposed folds are fold amplitude and fold tightness (GRUJIC, 1992). For a given early fold amplitude, compression parallel to the hinge lines of the first fold set ($F_1$) produces a transition in observed interference patterns from Type 1 to Type 2 with increasing tightness of early folds.

Field-based studies showing such interference relationships are not numerous. This is probably due to

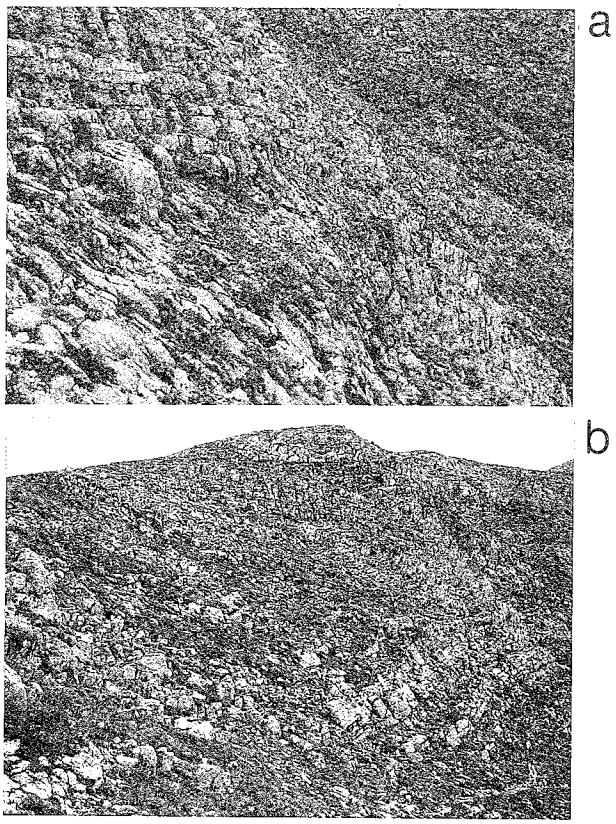


Fig. 36 - Gently inclined $F_1$ anticline in cherty limestones at thrust tip east of B' (cf. profile B-B''). (a) View approximately normal to $F_1$ axis (E is to the right). (b) Oblique view at a high angle to $F_2$ axis. Note elongated dome shape with major axis oriented roughly N-S.

the fact that most studies on superposed folding have been carried out in high grade metamorphic rocks. According to WATKINSON (1981), the best areas to observe the predominant mechanical effects of early folds on later folds are areas that do not have markedly high strain values, that is away from areas such as the deep-level interior zones of orogenic belts where bulk strain effects may predominate. The most common types of terrane to develop such features are those of rocks folded under low grade metamorphic conditions, where the bedding has a strong mechanical control on folding. One such area is in the Cantabrian Mountains of NW Spain, where large-scale interference patterns have been described (JULIVERT & MARCOS, 1973). These authors were able to show the difference in interference pattern between folds superposed on earlier tight antiforms and folds superposed on earlier open synforms. Basins (Type 1 patterns) form on open folds, whereas the axial planes of tight folds are folded, forming Type 2 patterns of interference (Fig. 40). Striking similarities with these patterns of interference are observed in the Lagonegro - M. Sirino area where, however, they are reversed due to earlier open antiforms and tight synforms, confirming the strong mechanical control exerted by the bedding during superposed folding at very low-grade conditions.

## KINEMATIC ANALYSIS OF THE LAGONEGRO AND ADJACENT NAPPES

As thrust faults related to $D_2$ shortening are not

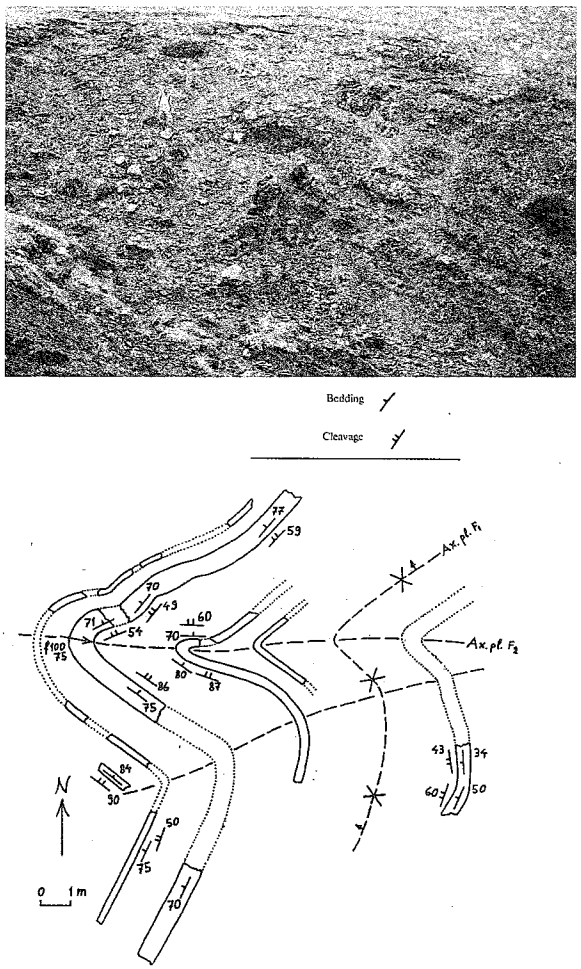


Fig. 37 - Type 2 interference patterns at Il Gavitone (Lower Cretaceous "Galestri"). (a) Steeply plunging $F_2$ folds superposed on the W overturned limb of $F_1$ syncline (N is to the right). (b) Schematic outcrop map (angle of dip of bedding and cleavage is indicated). As a result of refolding the steep western limb of $F_1$ shows a changing polarity in the three different sectors defined by $F_2$ axial planes. Bedding-cleavage relationships indicate a change of polarity from overturned to normal to overturned again moving from north to south.

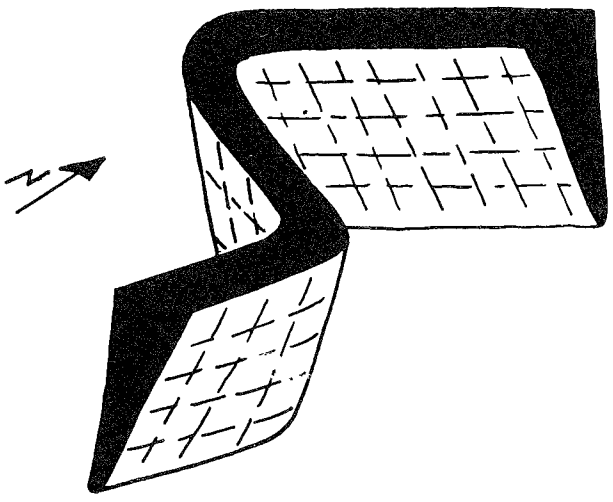

Fig. 38 - Schematic diagram of the refolds of Fig. 37.

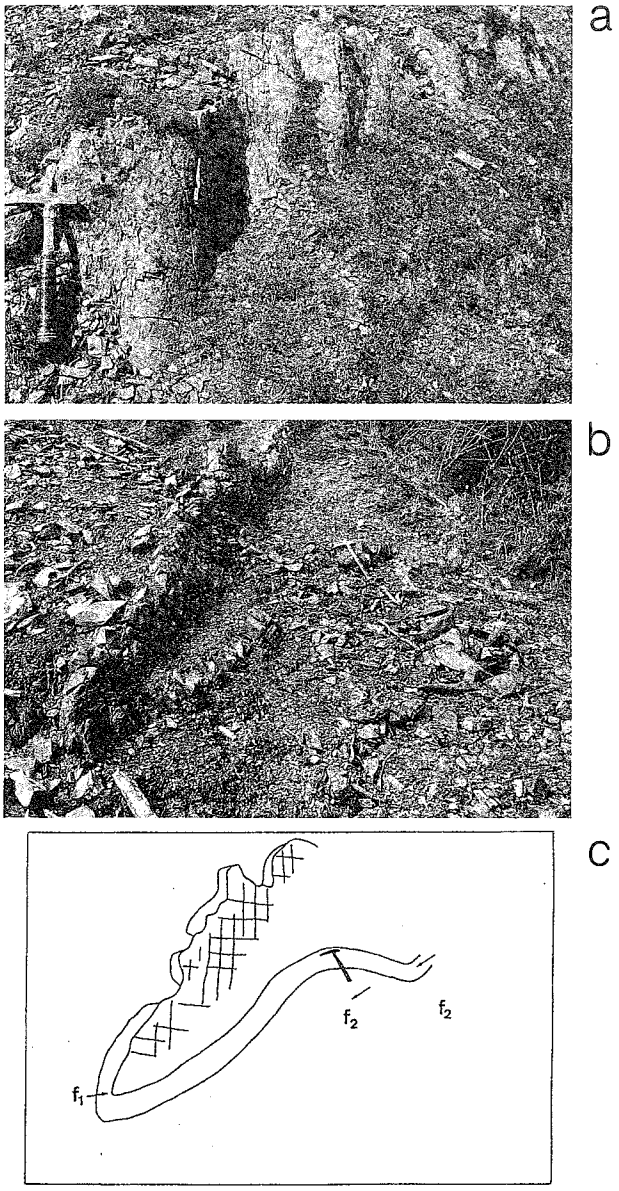


Fig. 39 - Minor structures associated with dominant Type 2 fold superposition. (a) Steeply plunging, upright open $F_2$ folds from the western limb of tight earlier syncline of Mad. di Sirino (NNW is to the right). Jurassic radiolarian cherts. (b) Upright open $F_2$ folds superposed on tight $F_1$ syncline, footwall of the thrust fault E of Serra Ortcosa (N is to the right). Lower Cretaceous "Galestri". (c) Line drawing from (b).

observed, the kinematic analysis is restricted to the main ($D_1$) deformation sequence. Thrust-related kinematic indicators are observed only at few localities from the main contact between the two Lagonegro nappes and from thrust faults within the lower nappe. Kinematic indicators from the M. Foraporta units outcropping in the western sector of the study area (Fig. 2) have also been included in the analysis (Fig. 41). The imbrication of these units probably also occurred within the $D_1$ deformation sequence, with a general transport direction towards the Apulian foreland.

Kinematic indicators may have been reoriented by later ($D_2$) deformation. Therefore, the data of Fig. 41 must be interpreted with caution, as it is not possible to specify to what extent later deformation influenced

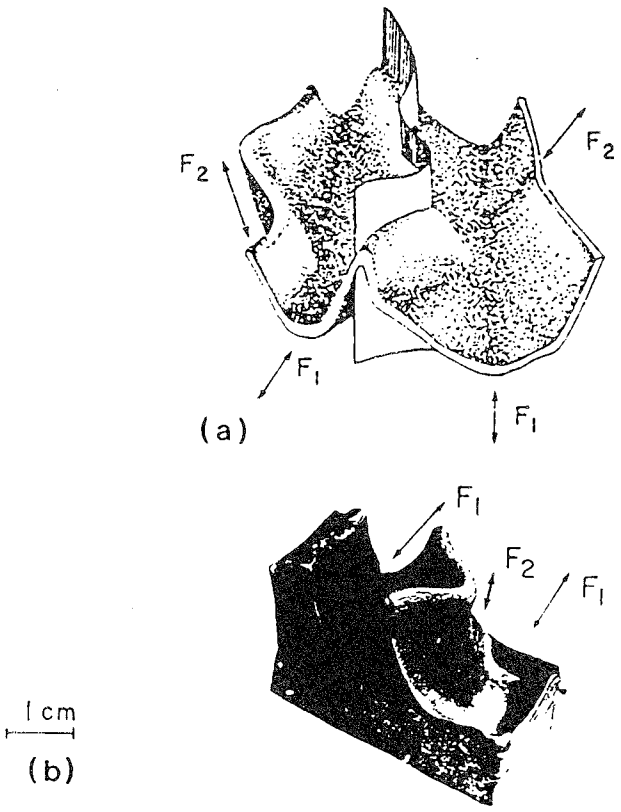


Fig. 40 - Superposed folding with Type 1 patterns on earlier open folds and Type 2 patterns on earlier tight folds (from Watkinson 1981). (a) Cantabrian refolds (cf. JULIVERT & MARCOS 1973). (b) Analogue model experiment (WATKINSON, 1981).

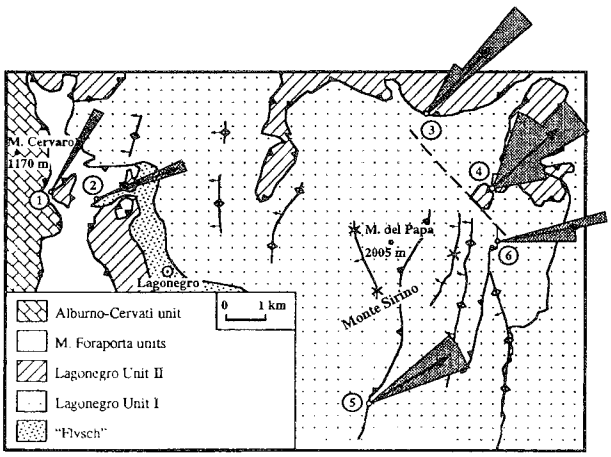


Fig. 41 - Thrust transport direction of the different tectonic units in the Lagonegro area (arrow indicates the relative movement of the upper block). Kinematic data are derived from shear bands, s-c tectonites, striae and shear vein fibres on fault planes. Data refer to: 1, 2, M.Foraporta Unit; 3, 4, Lagonegro Unit II; 5, 6, Lagonegro Unit I.

the primary range of movement directions. In any case, overthrusting directions reconstructed for the different tectonic units are reasonably consistent, varying from NNE- to ENE-oriented in present-day co-ordinates.

The kinematic indicators used at the different localities shown in Fig. 41 are briefly discussed below. The results of the kinematic analysis are summarized in Table 1.

*Monte Foraporta Unit*

West of the town of Lagonegro, Triassic-Jurassic carbonate slope or proximal basin sediments outcrop within a series of small tectonic slices intercalated between the Alburno-Cervati Unit (western platform) and the underlying Lagonegro units (Fig. 2).

The contact between the limestones of Tempa Pertusata slice and the black dolomites of Carcuni slice is well exposed along the road "S.S. delle Calabrie (N. 19)" at km 109, SSE of M. Cervaro. At this locality (site 1 in Fig. 41), calcite shear-vein fibres and striae on fault surface indicate an overthrusting direction to the NNE.

South of Tempa Foraporta (site 2 in Fig. 41) the black dolomites of Carcuni slice can be observed tectonically overriding the white dolomites of Nizzullo slice. The fault contact at this locality is very sharp and shows a highly polished and striated surface. Dolomites above and below the contact are strongly fractured and brecciated. Striae on the slickenside surface show an overthrusting direction to the ENE. It must be noted, however, that striations on slickensides generally record the last movement on the fault plane (e.g. RAMSAY & HUBER, 1987). These data must therefore be interpreted with caution.

*Lagonegro Unit II*

At Tempa di Roccarossa (site 3 in Fig. 41), several meters thick green chloritic claystones are found close to the basal thrust underlying the large neritic limestone block (M. Facito Fm.; Fig. 9). They show a well-developed shallow-dipping foliation and contain broken and often rotated fragments of laminated calcarenite, micaceous sandstone cobbles and rounded neritic limestone fragments. Many of the clasts show tails of calcite fibres developed in pressure shadows (Fig. 42a). The orientation of these fibres is parallel to that of the calcite fibre lineation observed on the foliation plane (i.e. NE-SW; Fig. 42b). These pressure-fringe structures show a very similar geometry to that of $\sigma_a$-type structures developed around porphyroclasts in mylonitic rocks (where, however, pressure shadow tails are dynamically recrystallized; e.g. PASSCHIER & SIMPSON, 1986). As in the case of $\sigma$-structures (Fig. 43), the tails on either side of the clast "step up" to the opposite side of the reference plane (parallel to the main foliation), so that an overall sigmoidal shape is attained (Figs. 42a, c & d). The asymmetry of the pressure shadows on either side of the clast is the result of a rotational deformation history and can serve as a valuable indicator of the sense of vorticity (MALAVIEILLE *et alii*, 1982). Deflection of the foliation occurs in a small distorted zone adjacent to the clast, where the foliation gradually changes in orientation to become roughly parallel to the clast margins in a similar fashion to that of Fig. 43b. The sense of shear given by these structures is invariably top to the NE. The same sense of shear is obtained by shear bands which deflect the foliation in the argillites (Fig. 44). These structures represent small-scale ductile shear zones that form within shear zones of larger dimensions. They are considered to represent one of the most reliable shear-sense indicators (SIMPSON & SCHMID, 1983). Shear bands form a weakly penetrative foliation at a low angle to a pre-

Table 1 - Thrust-related kinematic data from Lagonegro and adjacent nappes.

| Site | Tectonic unit | Lithology | Kinematic indicator | Movement direction of upper block (azimuth) |
|---|---|---|---|---|
| 1 | T. Pertusata | Limestones | Shear vein fibres, striae | 031° |
| 2 | Carcuni | Dolomites | Striae | 068° |
| 3 | Lagonegro II | Argillites | Shear bands, pressure fringes, shear vein fibres | 042° |
| 4 | Lagonegro II | Argillites<br>Limestones | Shear vein fibres<br>s-c tectonites | 049° |
| 5 | Lagonegro I | Argillites<br>Limestones | Shear bands<br>s-c tectonites, shear vein fibres | 063° |
| 6 | Lagonegro I | Argillites | Shear bands | 077° |

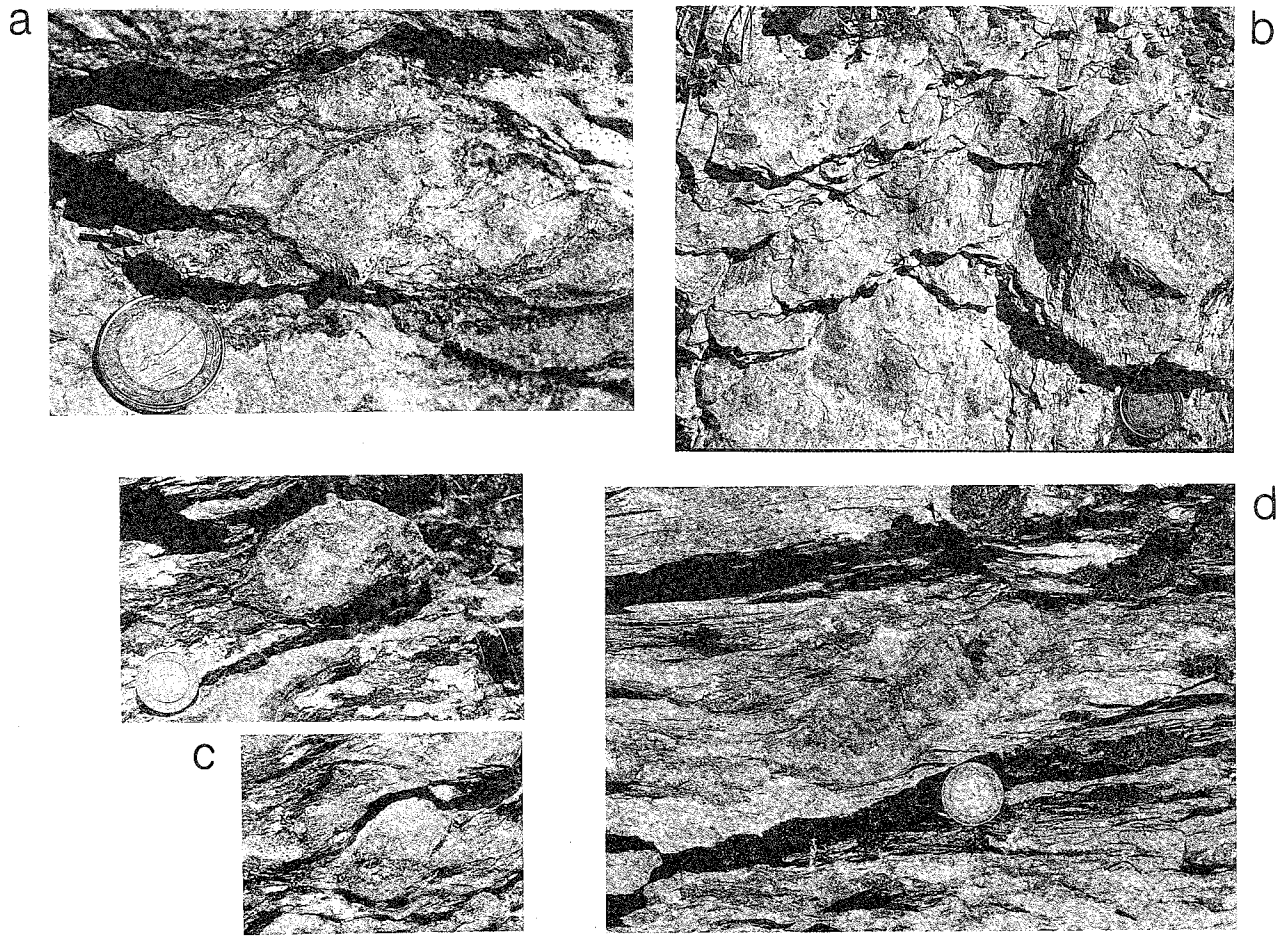


Fig. 42. Structural features from the shear zone at the base of Lagonegro Unit II at Tempa di Roccarossa (M. Facito Fm.) showing top-to-the-NE sense of shear (excluding (b), NE is to the right of all the pictures). (a) Calcite fibres (arrowed) at one end of a sigmoidally-shaped limestone clast (pressure-fringe structure). (b) Calcite shear vein fibres on foliation plane. (c) Ellipsoidal $\sigma_a$-type clasts. (d) Oblong $\sigma_a$-type clast.

existing foliation; the geometric relationship between the two foliations indicates the overall sense of shear. The intersection line between the early foliation and the shear bands is generally perpendicular to the stretching lineation in the rock (in the present case it is perpendicular to the mineral fibre lineation). Shear bands only occur locally, with limited lateral continuity, and never form a pervasive feature in rocks. They are considered to develop during the final stages of high-strain deformation in homogeneously foliated sheared rocks (White *et alii*., 1980; Simpson & Schmid, 1983). In the present case, the pre-existing foliation in the argillites is defined by a pervasive preferred orientation of phyllosilicates. In Fig. 44 it can be observed how the geometry of the clasts is modified by the heterogeneous fabric due to the development of the shear bands. The

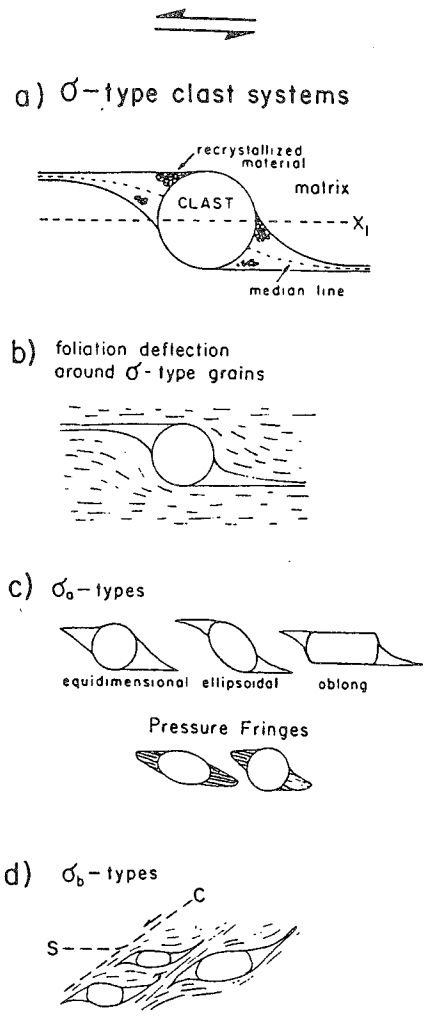


Fig. 43 - Geometry of $\sigma$-type porphyroclast systems with sinistral sense of vorticity (from Passchier & Simpson, 1986). (a) $\sigma$-type system ($X_1$ shows reference plane). (b) Foliation deflection around $\sigma$-type systems. (c) $\sigma_a$-type (equidimensional, ellipsoidal, oblong); pressure fringes. (d) $\sigma_b$-type associated with shear bands.

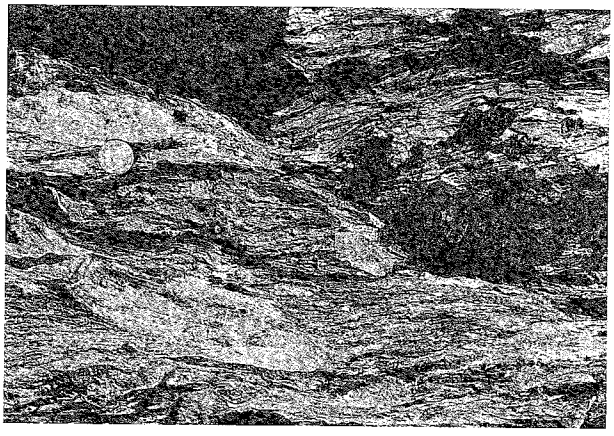

Fig. 44 - Shear bands (showing top-to-the-NE sense of shear) in green argillites of M. Facito Fm. close to the thrust contact at the base of Tempa di Roccarossa (NE is to the right of the picture). Note how the geometry of the clasts on the right side of the picture is influenced by the shear band fabric, attaining a $\sigma_b$-type geometry.

clasts are rotated and sheared along the NE-dipping shear bands, and attain a geometry similar to that of $\sigma_b$-type porphyroclast systems in mylonites (Fig. 43d).

Scattered E-W trending minor folds of centimetric amplitude are also observed folding the foliation in the argillites; they most probably relate to the later ($D_2$) contractional deformation phase.

The presence of a well-developed foliation and of shear bands in the argillites, together with the geometry of limestone and sandstone clasts imbedded in the matrix, suggest that these rocks have been strongly sheared. They are interpreted as the product of the deformation of terrigenous and calciclastic sediments of the lower M. Facito Fm. (cf. Wood,1981) within a several meters thick shear zone that developed at the base of the large neritic limestone block during nappe emplacement.

At Tempa S. Maria (site 4 in Fig. 41), the Upper Triassic "Calcari con selce" of Unit II overthrust the Lower Cretaceous "Galestri" of Unit I (Fig. 5). The argillites in the footwall show calcite shear vein fibres on the cleavage surface indicating NE-directed overthrusting. The shallow dipping limestones immediately above the thrust surface show a curved pressure solution cleavage which defines sigmoidally-shaped lithons. The overall geometry is similar to that of s-c structures (Berthé *et alii*, 1979; Simpson & Schmid, 1983; Lister & Snoke, 1984), with the sigmoidal pressure solution cleavage defining the s-structure and the shear banding (c-structure) being sub-parallel to bedding (which is, in turn, sub-parallel to the thrust plane).

*Lagonegro Unit I*

Although thrust faults within this unit are sometimes well exposed (Fig. 20a), reliable kinematic indicators have only been found at a few localities. One such locality is about 800 m NNE of the village of Varcovalle (site 5 in Fig. 41), along a thrust fault which brings the Upper Triassic "Calcari con selce" onto the Lower Cretaceous "Galestri" (Fig. 2). Here, calcite shear fibres and s-c tectonites are developed in the limestones in the hangingwall, indicating a relative movement of the upper block towards present-day ENE. In the "Galestri" of the footwall, shallow dipping shear bands are observed which deflect the $S_1$ slaty cleavage in the argillites. Although no mineral-fibre lineation is developed in these rocks, the movement direction of the shear bands is assumed to be approximately perpendicular to the intersection lineation of the shear bands and the $S_1$ cleavage. The constructed movement direction of the shear bands indicates an ENE overthrusting direction, consistent with that obtained from the limestones in the hangingwall.

Shear bands which deflect the S1 slaty cleavage in the argillites of the "Galestri" are observed also at site 6 of Fig. 41, in the footwall of the thrust fault east of Serra Orticosa (Fig. 2). The constructed movement direction for these shear bands indicates ENE-directed overthrusting.

## CONJUGATE SHEAR ZONES

Conjugate sets of en-echelon veins are observed at several localities in the Jurassic radiolarian cherts and more commonly in the Upper Triassic limestones. The veins generally lie at a high angle to the local bed-

ding. They are usually filled with calcite fibres in the limestones, whereas they can be either quartz- or calcite filled in the cherts. The arrays consist of straight (Fig. 45a) or, much more commonly, sigmoidally-shaped veins (Fig. 45b), showing the typical geometry of brittle-ductile shear zones; the conjugate relation-

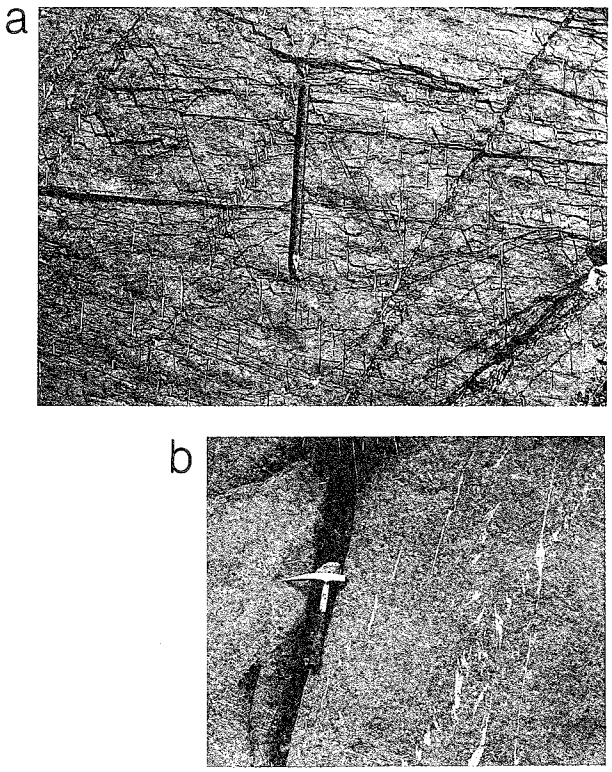

Fig. 45 - Conjugate sets of en-echelon calcite filled veins (N is to the left for both pictures). (a) Jurassic cherts along the road "S.S. delle Calabrie" west of Tempa Forapora. (b) Upper Triassic limestones ("Calcari con selce") SE of Mad. di Sirino.

ships can be used to evaluate the orientation of the bulk strain axes using the methods well established in the literature (RAMSAY & HUBER, 1987). The analysis has been carried out from locations where the two conjugate vein systems were equally developed, so that the maximum (X) and minimum (Z) bulk strains are found at the dihedral angle bisectors, and the intermediate axis (Y) is located at the intersection of the conjugate sets. The angle between the conjugate systems is quite variable, ranging from 20° to 73° (mean dihedral angle from 28 measured conjugate sets is 46°). The acute angle between the shear zones always faces the direction of bulk shortening determined from their relative sense of displacement. Orientation of the bulk shortening axes determined by this method throughout the whole study area are shown in Fig. 46. Two groups of conjugate shear zones have been distinguished on the basis of the bulk shortening direction indicated by them. Fig. 46a & b show roughly E-W and N-S shortening obtained from the analysis of groups 1 and 2, respectively. In a few cases, cross-cutting relationships between the two families could be observed, with conjugate shear zones belonging to group 2 overprinting zones related to group 1. This relative timing of shear zones development shows a general good agreement

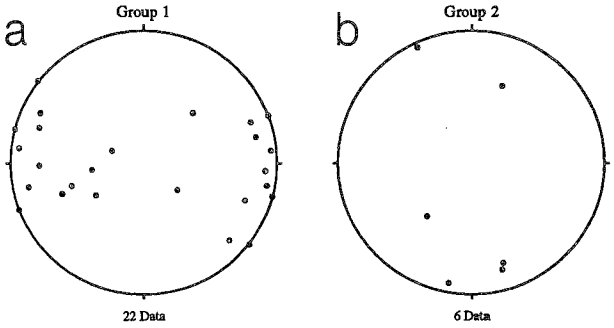


Fig. 46 - Orientation data for minimum bulk strain axis (Z) determined from the analysis of conjugate en-echelon vein systems (whole study area). (a) Data from group 1 shear zones. (b) Data from group 2 shear zones.

with the superposed $D_1$ and $D_2$ deformations described above. In most of the cases, however, only one of the two families is developed at each outcrop. In these cases the attribution to one or the other group of structures was based exclusively on orientation, and therefore must be taken with caution.

## FINITE STRAIN DATA

Finite strain states associated with the deformation have been measured from ellipsoidal iron-reduction bodies (e.g. WOOD *et alii*, 1976) which occur within the red mudstones at the base of the Jurassic radiolarian cherts (Fig. 47a). These natural strain indica-

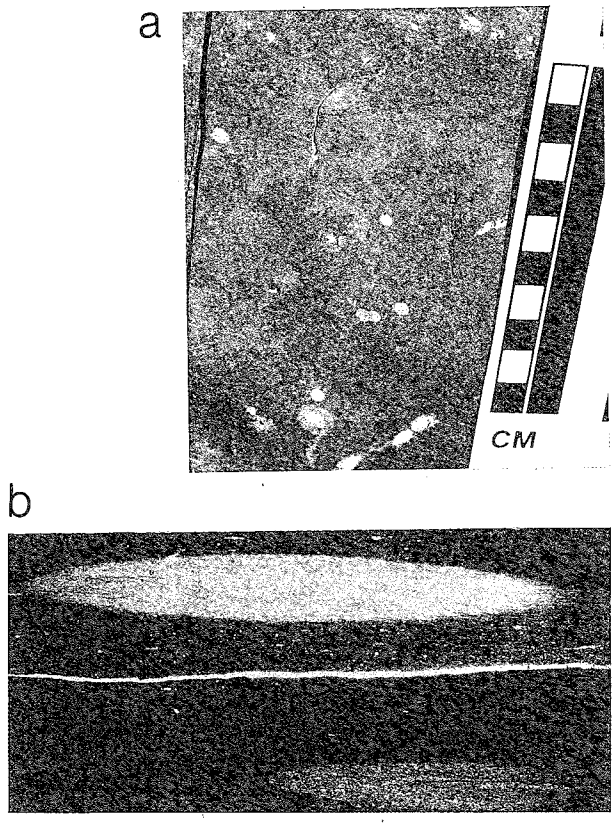


Fig. 47 - Reduction spots from red mudstones at the base of the Jurassic "Scisti silicei". (a) Cleavage surface (XY principal plane). (b) Thin section showing XZ principal plane.

tors are perfect triaxial ellipsoids which have their XY principal plane parallel to the plane of slaty cleavage, irrespective of the varying angular relations between the cleavage and the primary sedimentary layering. Their size varies in the study area from less than 1 millimeter to more than 1 centimeter across. According to WOOD *et alii* (1976) these indicators, first described as "reduction spots", are ellipsoidal bodies in which the total iron content of the rock is drastically depleted rather than being in a different oxidation state compared to the enclosing rock. The ellipsoids are the result of iron diffusion from point sources that are small compared to the volume of each ellipsoidal body. As such, they are at one end of a development spectrum, the opposite end of which consists of continuous planar zones of iron depletion along the primary sedimentary layering. Such zones, as well as discontinuous and irregular ones, are commonly observed in the red mudstones where the strain markers are found. The iron which has been depleted was mainly fine-grained haematite and its removal permits the otherwise masked pale green colour of chlorite to contrast with the purple and red colours of the non-depleted bulk of the rock.

*Methodology*. - Surfaces parallel to the cleavage were first analysed in order to determine the exact orientation of the long (X) and intermediate (Y) axes of the finite strain ellipsoid. The deformed reduction bodies were analysed with a Macintosh based digitization and morphology measurement system - Image Analyst (v. 7.2, Automatix Inc, Billerica, Mass., USA). This system, originally developed for and often employed in industrial robot vision applications, automatically detects the exterior outlines of objects and generatesit large suite of morphology metrics for each outline detected. A subset of these parameters was used for strain determinations: axial ratio ($R_f$) and orientation ($\phi$) of the longest diameter with respect to the strike of the cleavage. Mean ellipticity ($R_s$) was determined by the harmonic mean (H) of the measured axial ratios ($R_f$) (e.g. RAMSAY & HUBER, 1983; LISLE, 1985)

$$H = N / \sum_{N}^{1} R_f^{-1}$$

while the vector mean $\phi$ was obtained according to LISLE (1985):

$$\bar{\phi} = \frac{1}{2} \arctan \left( \sum_{N}^{1} \sin 2\phi \; / \; \sum_{N}^{1} \cos 2\phi \right)$$

The specimens were subsequently cut normal to the cleavage and parallel to the maximum extension direction determined as above in order to perform image analysis and $R_f/\phi$ measurements on the XZ principal section of the finite strain ellipsoid (Fig. 47b).

*Results*. - Three-dimensional finite strain data determined from different sites in the M. Sirino group (Lagonegro Unit I) are shown in Table 2 (parameters of individual ellipses measured by image analysis are listed in Mazzoli, 1993a). The measured strains appear not to be influenced by the later ($D_2$) deformation as: (1) no $S_2$ fabrics were observed deforming $S_1$ from the sites where the spots were sampled, (2) the XY principal plane of the finite strain ellipsid is always parallel to the $S_1$ cleavage.

Most of the data plot in the apparent flattening field (Fig. 48). Dip angle (Table 2) of the maximum extension direction (X) varies from 3° to 50°, but is generally shallow (mean = 21°, standard deviation *s*

Table 2 - Finite strain data from reduction spots. $X \geq Y \geq Z$ are the principal axes of the finite strain ellipsoid. $\phi$ is the angle between X and the strike of the cleavage (anticlockwise: + ve, clockwise: -ve). $K = (\epsilon_1 - \epsilon_2)/(\epsilon_2 - \epsilon_3)$; $D = [(\epsilon_1 - \epsilon_2)^2 + (\epsilon_2 - \epsilon_3)^2]^{1/2}$.

| Sample | Cleavage attitude | Axis orientation X | Y | Z | $\phi$ (deg) | Axis ratio X : Y : Z | K | D |
|---|---|---|---|---|---|---|---|---|
| S8 | 275/38 | 189/03 | 282/38 | 095/52 | 4 | 1.32 : 1 : 0.41 | 0.32 | 0.92 |
| S107 | 155/12 | 175/12 | 075/02 | 335/78 | -70 | 2.14 : 1 : 0.33 | 0.69 | 1.34 |
| S149 | 295/50 | 295/50 | 025/00 | 115/40 | 89 | 2.46 : 1 : 0.38 | 0.93 | 1.32 |
| S154 | 050/80 | 323/19 | 113/69 | 230/10 | 19 | 1.46 : 1 : 0.50 | 0.54 | 0.79 |
| S155 | 245/48 | 312/24 | 202/40 | 065/42 | -31 | 1.85 : 1 : 0.54 | 1.00 | 0.87 |
| S156 | 265/55 | 353/03 | 260/55 | 085/65 | -3 | 1.46 : 1 : 0.30 | 0.31 | 1.26 |
| S158 | 252/58 | 313/37 | 189/37 | 072/32 | -44 | 1.32 : 1 : 0.19 | 0.17 | 1.65 |
| S159 | 245/65 | 173/33 | 305/47 | 065/25 | 35 | 1.49 : 1 : 0.56 | 0.70 | 0.70 |
| S160 | 270/40 | 201/18 | 304/34 | 090/50 | 26 | 2.05 : 1 : 0.89 | 6.24 | 0.73 |
| S161 | 230/38 | 311/06 | 216/37 | 050/52 | -9 | 2.63 : 1 : 0.57 | 1.73 | 1.12 |
| S162 | 235/32 | 292/18 | 194/25 | 055/58 | -34 | 1.52 : 1 : 0.44 | 0.51 | 0.91 |
| S164 | 245/68 | 175/40 | 314/42 | 065/22 | 42 | 1.42 : 1 : 0.58 | 0.65 | 0.64 |
| S165 | 237/20 | 192/15 | 286/13 | 057/70 | 44 | 2.08 : 1 : 0.52 | 1.14 | 0.97 |
| S166 | 260/26 | 210/18 | 305/18 | 080/64 | 40 | 1.66 : 1 : 0.40 | 0.55 | 1.05 |
| S168 | 198/43 | 279/09 | 181/42 | 048/17 | -12 | 1.53 : 1 : 0.46 | 0.54 | 0.89 |
| S172 | 210/50 | 256/40 | 143/26 | 030/40 | -56 | 1.61 : 1 : 0.60 | 0.92 | 0.70 |

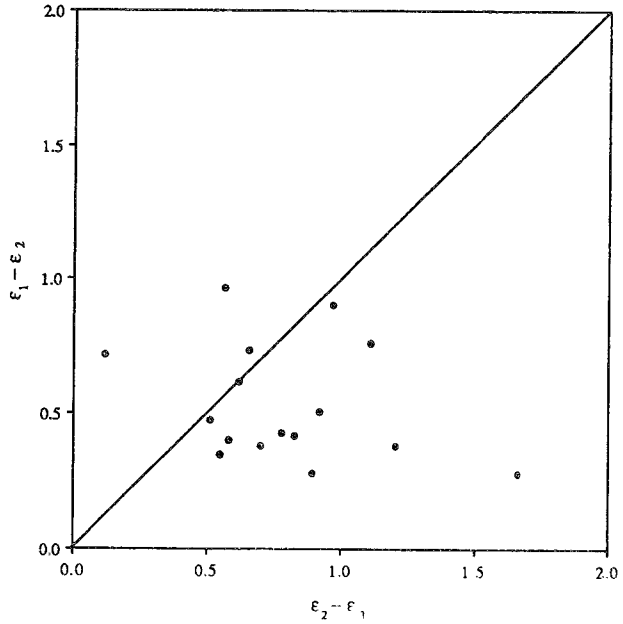


Fig. 48 - Logarithmic deformation plot of finite strain data from reduction spots. $\epsilon_1$-$\epsilon_2$ = ln $R_{XY}$; $\epsilon_2$-$\epsilon_3$ = ln $R_{YZ}$.

= 14°). The intermediate (Y) axis shows a mean dip of 33° and a larger variability ($s$ = 18°), while the minimum extension (Z) is generally moderately plunging (mean = 45°, $s$ = 20°). Considering such orientation features, the representation of the finite strains has been carried out by drawing the shapes of the XY principal plane strain ellipses on the map (Fig. 49). As the intermediate (Y) axis is generally not sub-horizontal and shows a variable dip, the angle of dip of the Y axis is shown beside the corresponding ellipse. In Fig. 3.48 it can be seen that there is a tendency for the maximum extension direction (X) to align either sub-parallel or sub-perpendicular to the main structural trends (axial traces, thrust faults). Therefore, the shapes of either the XZ or the YZ principal plane strain ellipses is represented in cross-section (Fig. 50), depending on the orientation of the X axis (sub-parallel or sub-perpendicular to the profile, respectively).

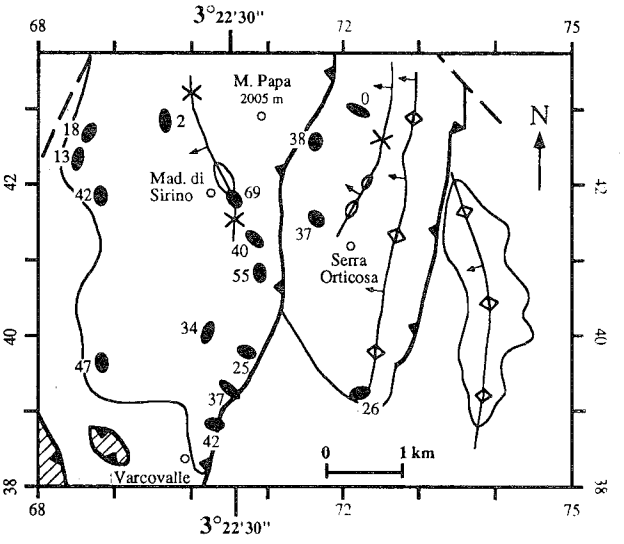


Fig. 49 - Map showing the shapes of XY principal plane strain ellipses from the area of M. Sirino. The angle of dip of the intermediate (Y) axis is shown beside each ellipse (on the side of the direction of dip).

*Discussion.* - The strain features shown in Figs. 49 & 50 do not allow a simple strightforward interpretation. Although they do not appear to record any $D_2$-related deformation, measured finite strains probably do reflect superposed deformations. In fact, the data were obtained from mudstone lithologies in which compactional effects may have a major influence on finite strain states (OERTEL, 1970; RAMSAY & WOOD, 1973; SANDERSON, 1976; RAMSAY & HUBER, 1983; BEUTNER & CHARLES, 1985; WRIGHT & HENDERSON, 1992). As has been observed above, a pattern to the orientation of the maximum extension axis (X) can be recognized, as it tends to align either sub-parallel or sub-perpendicular to the main structures. A more detailed analysis has been carried out by measuring the angle between the X direction of the finite strain ellipsoid and the local fold axis (given by the bedding-cleavage intersection lineation) at each locality (Fig. 51). This angle shows a roughly bimodal distribution, confirming the general trends observed on the map of Fig. 49. This type of distribution, with maxima at a low and at a high angle to the local fold axes, can be the result of a deformational history involving the superposition of tectonic strain on consistent volume loss related to diagenetic compaction (MAZZOLI & CARNEMOLLA, 1993). This type of superposition may also account for the oblate shape of most of the measured finite strain ellipsoids (Fig. 48). It has to be noted, however, that locally a component of true tectonic extension sub-parallel to the fold axes cannot be ruled out. Definite evidence on this point is lacking as no absolute length change markers were available.

## SUMMARY AND CONCLUDING REMARKS

Fieldwork in the Lagonegro - M. Sirino area has allowed the reconstruction of a structural evolution involving a sequence of superposed deformations. The main points of such evolution are summarized below.

(1) The earliest deformation recorded by the Mesozoic Lagonegro sediments is that related to diagenetic compaction. This is important especially in the less competent lithologies (mudstones and argillites), as shown by the finite strain data above and by the deformation fabrics (MAZZOLI & CARNEMOLLA, 1993).

(2) Folding in the upper Lagonegro unit (II) appears to have been essentially coeval with nappe emplacement, as shown by the relation between fold geometry and structural position within the nappe.

(3) The main nappe contact is itself gently bowed, but is discordant to the structures in the footwall. Locally it also cuts down-section in the direction of transport into the underlying Lagonegro Unit I. When the results of the kinematic analysis of the present study are considered, such out-of-sequence features can be observed also from the map and the profiles of TORRENTE (1990) from an adjacent area north of M. Gurmara, and from SCANDONE (1972) on a more regional scale. The gentle folds defined by the thrust surface roughly show a correspondence to structures in the

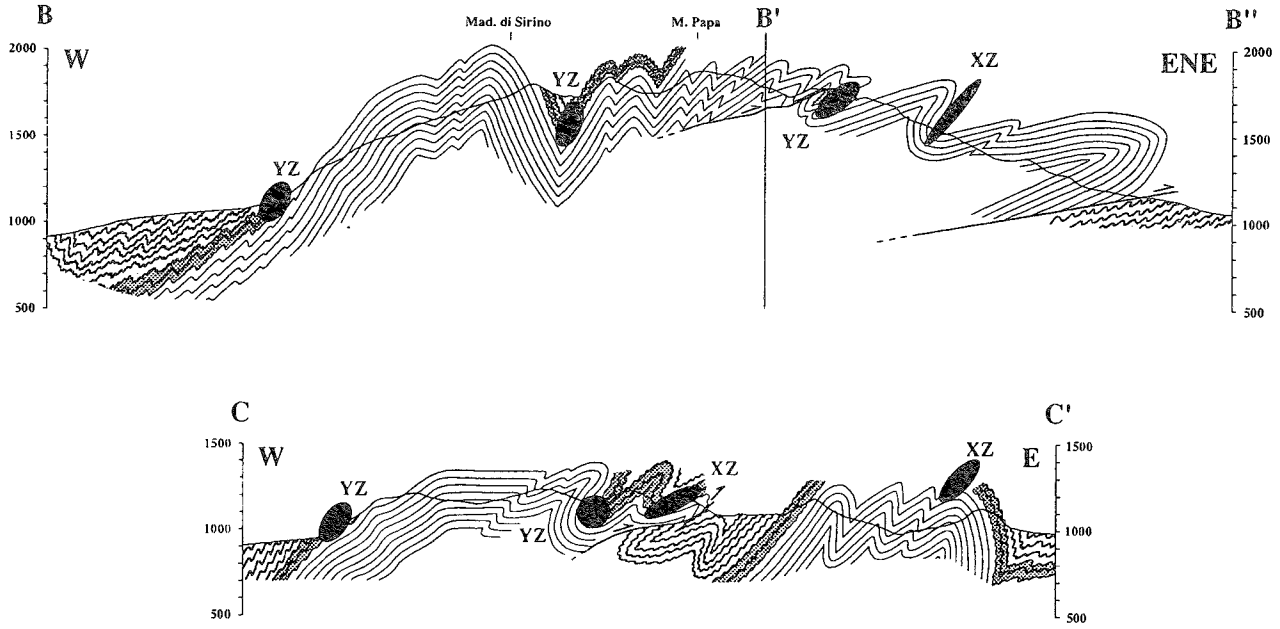


Fig. 50 - Cross-sections showing the shapes of the XZ or YZ (indicated) principal plane strain ellipses.

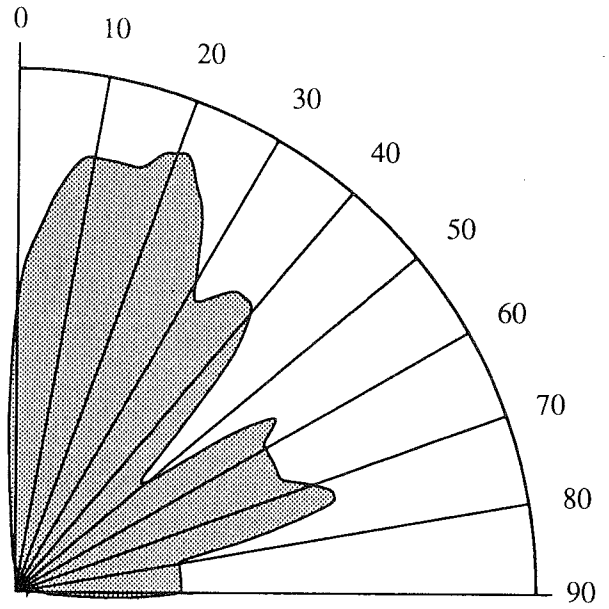


Fig. 51 - Angle between axis of maximum finite extension (X) and bedding-cleavage intersection lineation measured at each locality in Fig. 49.

footwall, although folds in the footwall are much tighter. For instance, the klippe between M. Gurmara and M. Niella is preserved in a syncline of the underlying Lagonegro Unit I (profile A-A' in Fig. 4). All these features suggest that folding within the lower nappe (Unit I) was also essentially coeval with the emplacement of the upper nappe. Movement of Unit II over an already deforming footwall would have caused the observed cut-off relationships of the nappe contact at different stratigraphic levels in the footwall. Continued fold development and tightening led to gentle folding of the thrust surface itself.

(4) Further thrusting occurred within Lagonegro Unit I, involving faulting of already folded rocks with only limited displacements compared to the main nappe transport. Where such displacements were more consistent, however, fold geometry appears to have been modified by movement over the thrust surfaces: folds tighten and axial planes become progressively shallower towards the thrust tip-line (profile B-B' in Fig. 4).

(5) Kinematic analysis of the Lagonegro and adjacent nappes indicates (present-day) E- to NE-directed overthrusting throughout the whole deformation sequence ($D_1$) described in (2) to (4) above.

(6) Refolding of the whole tectonic pile occurred as a consequence of (present-day) N-S to NNE-SSW shortening ($D_2$). This event produced different types of interference structures at various scales. The most commonly observed are transitional forms between Type 1 and Type 2 interference patterns of RAMSAY (1967). Although these are complex structures that never represent simple end-members, at a first approximation a pattern can be recognized consisting of (dominant Type 1) dome-like structures developed on early broad anticlines and of (dominant Type 2) tight synclinal structures with folded axial surfaces developed on early "pinched" synclines.

(7) Folding of the axial surfaces of early structures is at least partly responsible for the markedly arcuate $F_1$ structural trends. It must be noted, however, that it is not possible to determine how much of this curvature was preexisting (i.e. related to $D_1$ thrusting), and how much was accentuated or newly formed by $D_2$-related strains.

ACKNOWLEDGEMENTS

I am grateful to JOHN RAMSAY, NEIL MANCKTELOW and DANIEL BERNOULLI for many stimulating discussions both in the field and at the Institute, and for carefully revising the manuscript. Many thanks are also due to DOROTHEE DIETRICH, DJORDJE GRUJIC and ADRIAN PFIFFNER for their useful comments and suggestions, and to URS GERBER for the preparation of the photographic material. Financial support from the ETH Zürich is gratefully acknowledged.

REFERENCES


BERNOULLI D. & JENKINS H.C. (1974) - *Alpine, Mediterranean and Central Atlantic Mesozoic facies in relation to the early evolution of the Tethys. In: Modern and ancient geosynclinal sedimetnation* (edited by R.H. Dott & R.H. Shaver). Soc. Econ. Paleont. Miner. Spec. Publ. **19**, 129-160.

BERNOULLI D., WEISSERT, H. & BLOME C.D. (1990) - *Evolution of the Triassic Hawasina basin, Central Oman Mountains*. In: (edited by A.H.F. Searle and A.C. Ries) *The Geology and Tectonics of the Oman Region*. Geol. Soc. Spec. Publ. **49**, 189-202.

BERTHÉ D., CHOUKROUNE P. & JEGOUZO P. (1979) - *Orthogneiss, mylonite and noncoaxial deformation of granites: the example of the South Armorican shear zone*. J. Struct. Geol. **1**, 31-42.

BEUTNER E.C. & CHARLES E.G. (1985) - *Large volume-loss during cleavage formation, Hamburg sequence, Pennsylvania*. Geology **13**, 803-805.

BOUILLIN J.P., DURAND-DELGA M. & OLIVIER P. (1986) - *Betic-Rifian and Tyrrhenian arcs: distinctive features, genesis and development stages*. In: *The Origin of Arcs* (edited by F.C. Wezel). Elsevier, Amsterdam, 281-304.

BOYER S.E. & ELLIOTT D. (1982) - *Thrust systems*. Bull. Am. Ass. Petrol. Geol. **66**, 1196-1230.

BRYANT B. & REED J.C.J. (1969) - *Significance of lineation and minor folds near major thrust faults in the southern Appalachians and the British and Norwegian Caledonides*. Geol. Mag. **106**, 412-429.

CASERO P., ROURE F., MORETTI I., MÜLLER C., SAGE L. & VIALLY R. (1988) - *Evoluzione geodinamica neogenica dell'Appennino meridionale*. Atti 74° Congr. Soc. Geol. Ital., Riassunti B, 59-66.

CHANNELL J.E.T., D'ARGENIO B. & HORVATH F. (1979) - *Adria, the African promontory, in Mesozoic Mediterranean paleogeography*. Earth Sci. Rev. **15**, 213-292.

CHEENEY R.F. (1983) - *Statistical Methods in Geology*. George Allen & Unwin, London.

CINQUE A., PATACCA E., SCANDONE P. & TOZZI M. (in press) - *Quaternary kinematic evolution of the Southern Apennines. Relationships between surface geological features and deep lithospheric structures*. In: *Atti International School on Solid Earth geophysics,* "Modes of crustal deformation from the brittle upper crust through detachments to the lower crust", Erice (TP).

COBBOLD P.R. (1976) - *Mechanical effects of anisotropy during large finite deformations*. Bull. Soc. géol. France **7**, 1497-1510.

COOPER M.A. & TRAYNER P.M. (1986) - *Thrust-surface geometry: implications for thrust-belt evolution and section-balancing techniques*. J. Struct. Geol. **8**, 305-312.

COSGROVE J.W. (1976) - *The formation of crenulation cleavage*. J. Geol. Soc. Lond. **132**, 155-178.

COWARD M.P. & KIM J.H. (1981) - *Strain within thrust sheets*. In: *Thrust and Nappe Tectonics* (edited by K.R. McClay and N.J. Price), Geological society Special Publication **9**, 275-292.

COWARD M.P. & POTTS G.J. (1983) - *Complex strain patterns developed at the frontal and lateral tips to shear zones and thrust zones*. J. Struct. Geol. **5**, 383-399.

DAHLSTROM C.D.A. (1970) - *Structural geology in the eastern margin of the canadian Rocky Mountains*. Bull. Can. Petrol. Geol. **18**, 332-406.

DE ALFIERI A., GUZZI R., SACCHI M., D'ARGENIO B. & ZAMPARELLI V. (1986) - *Monte Foraporta Unit: a minor element of southern Apennine nappe pile, stratigraphic and tectonic study*. Rend. Soc. Geol. Ital. **9**, 171-178.

DE SITTER L.U. (1952) - *Plissement croisé dans le Haut Atlas*. Geol. Mijnbouw **14**, 277-282.

DIETRICH D. (1988) - *Sense of overthrust shear in the Alpine nappes of Calabria (Southern Italy)*. J. Struct. Geol. **10**, 373-381.

ELLIOTT D. (1976) - *The energy balance and deformation mechanisms of thrust sheets*. Phil. Trans. R. Soc. London **282**, 289-312.

ESCHER A. & WATTERSON J. (1974) - *Stretching fabrics, folds and crustal shortening*. Tectonophysics **22**, 223-231.

FISCHER M.P., WOODWARD N. & MITCHELL M.M. (1992) - *The kinematics of break-thrust folds*. J. Struct. Geol. **14**, 451-460.

FISCHER M.W. & COWARD M.P. (1982) - *Strains and folds within thrust sheets: an analysis of the heilam sheet, northern Scotland*. Tectonophysics **88**, 291-312.

GHOSH S.K., MANDAL N., KHAN D. & DEB S.K. (1992) - *Modes of superposed folding in single layers controlled by initial tightness of early folds*. J. Struct. Geol. **14**, 381-394.

GRAY D.R. (1977a) - *Morphologic classification of of crenulation cleavages*. J. Geol. **85**, 229-235.

GRAY D.R. (1977b) - *Some parameters which affect the morphology of crenulation cleavages*. J. Geol. **85**, 763-780.

GRAY D.R. (1979a) - *Microstructure of crenulation cleavages: an indicator of cleavage origin*. Am. J. Sci. **279**, 97-128.

GRAY D.R. (1979b) - *Geometry of crenulation-folds and their relationship to crenulation cleavage*. J. Struct. Geol. **1**, 187-205.

GRAY D.R. & DURNEY D.W. (1979) - *Investigations on the mechanical significance of crenulation cleavage*. Tectonophysics **58**, 35-79.

GRUJIC, D. (1992) - *Superposed folding: analogue models and comparison with natural examples from the maggia nappe (Pennine Zone, Switzerland)*. Unpublished D. Phil. thesis, ETH Zürich.

HILL K.C. & HAYWARD A.B. (1988) - *Structural constraints on the tertiary plate tectonic evolution of Italy*. Marine and Petroleum Geology **5**, 2-16.

HIPPOLYTE J.C., ANGELIER J., ROURE F. & BARRIER E. (1991) - *Paleostress reconstructions in Southern Apennines*. Terra Abstracts **1**, 259.

JAMISON W.R. (1987) - *Geometric analysis of fold development in overthrust terranes*. J. Struct. Geol. **9**, 207-219.

JULIVERT M. & MARCOS A. (1973) - *Superimposed folding under flexural conditions in the Cantabrain Zone (Hercynian Cordillera, northwest Spain)*. Am. J. Sci. **273**, 353-375.

KNOTT S.D. (1987) - *The Liguride Complex of Southern Italy - a Cretaceous to Paleogene accretionary wedge*. Tectonophysics **142**, 217-226.

LAUBSCHER H. & BERNOULLI D. (1977) - *Mediterranean and Tethys*. In: *The Ocean Basins and Margins* (edited by E.M. Nairn and W.H. Kanes). Plenum Press, New York, 1-28.

LAUBSCHER H.P. (1976) - *Geometrical adjustments during rotation of a Jura fold limb*. Tectonophysics **36**, 347-365.

LENTINI F., CARBONE S., CATALANO S. & MONACO C. (1990) - *Tettonica a thrust neogenica nella catena appenninico-maghrebide: esempi dalla Lucania e dalla Sicilia. Studi Geologici Camerti, Volume speciale (1990), 19-26*.

LISLE R.J. (1985) - *Geological Strain analysis. A Manual for the $R_f/f$ Method*. Pergamon Press, Oxford.

LISLE R.J., STYLES P. & FREETH S.J. (1990) - *Fold interference structures: the influence of layer competence contrast*. Tectonophysics **172**, 197-200.

LISTER G.S. & SNOKE A.W. (1984) - *S-C mylonites*. J. Struct. Geol. **6**, 617-638.

MALAVIEILLE J., ETCHECOPAR A. & BURG J.P. (1982) - *Analyse de la géométrie des zones abriées: simulation et application à des example naturels*. C.R. Acad. Sc. Paris **294**, 279-284.

MANCKTELOW N.S. (1981) - *A least square method for determining the best-fit point maximum, great circle, and small circle to nondirectional orientation data*. Math. Geol. **13**, 507-521.

MAZZOLI S. (1993a) - *Structural analysis of the Mesozoic Lagonegro Units in SW Lucania, southern Apennines, Italy*. Unpublished D. Phil. thesis, ETH Zurich.

MAZZOLI, S. (1993b) - *Low-temperature deformation of fine grained limestones and quartzites, Lagonegro basin Mesozoic succession (southern Apennines, Italy)*. Annales Tectonicae **13**(1), in press.

MAZZOLI S. & CARNEMOLLA S. (1993) - *Effects of the superposition of compaction and tectonic strain during folding of a multilayer sequence - model and observations*. J. Struct. Geol., **15**, 277-291.

MEANS W.D. (1976) - *Stress and Strain*. Springer-Verlag, New York.

MOSTARDINI F. & MERLINI S. (1986) - *Appennino centro meridionale. Sezioni geologiche e proposta di modello strutturale*. AGIP, 73 Congresso Societa Geologica Italiana, Roma, 1-59.

OERTEL G. (1970) - *Deformation of a slaty lapillar tuff in the English Lake District*. Geol. Soc. Am. Bull. **78**, 1173-1187.

OGNIBEN L. (1969) - *Schema introduttivo alla geologia del confine calabro-lucano*. Mem. Soc. Geol. Ital. **8**, 453-763.

PASSCHIER C.W. & SIMPSON C. (1986) - *Porphyroclast systems as kinematic indicators*. J. Struct. Geol. **8**, 831-843.

PATERSON S.R. (1989) - *A reinterpretation of conjugate folds in the central Sierra Nevada, california*. Bull. geol. Soc. Am. **101**, 248-259.

POWELL C.M. (1979) - *A morphological classification of rock cleavage*. Tectonophysics **58**, 21-34.

RAMSAY G.J. & WOOD D.S. (1973) - *The geometric effects of volume*

*change during deformation processes.* Tectonophysics **16**, 263-277.

RAMSAY J.G. (1962) - *The geometry of conjugate fold systems.* Geol. Mag. **99**, 516-526.

RAMSAY J.G. (1967) - *Folding and fracturing of rocks.* McGraw Hill, New York.

RAMSAY J.G. (1981) - *Tectonics of the Helvetic Nappes.* In: *Thrust and Nappe Tectonics* (edited by K.R. McClay and N.J. Price), Geol. Soc. Spec. Publ. **9**, 293-309.

RAMSAY J.G. (1989) - *Fold and fault geometry in the western Helvetic nappes of Switzerland and France and its implication for the evolution of the arc of the western Alps.* In: *Alpine Tectonics* (edited by M.P. Dietrich and R.G. Park), Geol. Soc. Spec. Publ. **45**, 33-45.

RAMSAY J.G. (1992) - *Some geometric problems of ramp-flat thrust models.* In: *Thrust Tectonics* (edited by K.R. McClay). Chapman & Hall, London, 191-200.

RAMSAY J.G., CASEY M. & KLIGFIELD R. (1983) - *Role of shear in development of the Helvetic fold-thrust belt of Switzerland.* Geology **11**, 439-442.

RAMSAY J.G. & GRAHAM R.H. (1970) - *Strtain variations in shear belts.* Can. J. Earth Sci. **7**, 786-813.

RAMSAY J.G. & HUBER M.I. (1983) - *The Techniques of Modern Structural geology, Volume 1, Strain Analysis.* Academic Press, London.

RAMSAY J.G. & HUBER M.I. (1987) - *The Techniques of Modern Structural Geology, Volume 2, Folds and Fractures.* Academic Press, London.

RICH J.L. (1934) - *Mechaniçs of low-angle overthrust faulting as illustrated by Cumberland thrust block, Virginia, Kentucky and Tennessee.* Bull. Am. Ass. Petrol. Geol. **18**, 1584-1596.

ROURE F., CASERO P. & VIALLY R. (1991) - *Growth processes and melange formation in the southern Apennines accretionary wedge.* Earth and Planetary Science Letters **102**, 395-412.

SANDERSON D.J. (1973) - *The development of fold axes oblique to the regional trend.* Tectonophysics **16**, 55-70.

SANDERSON D.J. (1976) - *The superposition of compaction and plain strain.* Tectonophysics **30**, 35-54.

SANDERSON J.D. (1982) - *Models of strain variation in nappes and thrust sheets: a review.* Tectonophysics **88**, 201-233.

SCANDONE P. (1967) - *Studi di geologia lucana: la serie calcareo-silico-marnosa e i suoi rapporti con l'Appennino calcareo.* Boll. Soc. Natur. Napoli **76**, 1-175.

SCANDONE P. (1972) - *Studi di geologia lucana: carta dei terreni della serie calcareo-silico-marnosa e note illustrative.* Boll. Soc. Natur. Napoli **81**, 225-300.

SCANDONE P. (1975a) - *Triassic seaways and the Jurassic Tethys Ocean in the central Mediterranean area.* Nature **256/5513**, 117-119.

SCANDONE P. (1975b) - *The preorogenic history of the Lagonegro basin (Southern Apennines).* In: *Geology of Italy* (edited by C. Squyres), The Earth Sciences Society of the Libyan Arab Republic, Tripoli, 305-315.

SIMPSON C. & SCHMID S. (1983) - *An evaluation of criteria to deduce the sense of movement in sheared rocks.* Geol. Soc. Am. Bull. **94**, 1281-1288.

STAMPFLI G.M., MARCOUX J. & BAUD A. (1991) - *Tethyan margin in space and time.* In: *Palaeogeography and Palaeooceanography of Tethys* (edited by J.E.T. Channell, E.L. Winterer & L.F. Jansa), Palaeogeogr., Palaeoecol., Plaeoclim. **87**, 373-409.

STUBLEY M.P. (1990) - *The geometry and kinematics of a suite of conjugate kink bands, southeastern Australia.* J. Struct. Geol. **12**, 1019-1031.

SUPPE J. (1983) - *Geometry and kinematics of fault-bend folding.* Am. J. Sci. **283**, 684-721.

SUPPE J. (1985) - *Principles of Structural Geology.* Prentice Hall, New Jersey.

TORRENTE M.M. (1990) - *Evoluzione strutturale delle successioni calcareo-silico-marnose nei dintorni di Lagonegro.* Unpublished D. Phil. thesis, Università di Napoli.

WATKINSON A.J. (1981) - *Patterns of fold interference: influence of early fold shapes.* J. Struct. Geol. **3**, 19-23.

WHITE S., BURROWS S. & CARREREAS J. (1980) - *Mylonites in ductile shear zones.* J. Struct. Geol. **2**, 175-178.

WOOD A.W. (1981) - *Extensional tectonics and the birth of the Lagonegro basin (southern Italian Apennines).* N. Jb. Geol. Pal. Abh. **161**, 93-131.

WOOD D.S., OERTEL G., SINGH J. & BENNETT H.F. (1976) - *Strain and anisotropy in rocks.* Phil. Trans. R. Soc. Lond. A **283**, 27-42.

WRIGHT T.O. & HENDERSON J.R. (1992) - *Volume loss during cleavage formation in the Meguma Group, Nova Scotia, Canada.* J. Struct. Geol. **14**, 281-290.